GEOLOGY OF THE UPPER SOUTHWEST RIFT ZONE OF HALEAKALA VOLCANO, MAUI, HAWAII

A THESIS SUBMITTED TO THE GRADUATE DIVISION OF THE UNIVERSITY OF HAWAII IN PARTIAL FULFILLMENT OF THE REQUIREMENTS FOR THE DEGREE OF

MASTER OF SCIENCE

IN GEOLOGY AND GEOPHYSICS

AUGUST 1977

By

Keith Alan Horton

Thesis Committee:

Gordon A. Macdonald, Chairman
Ralph Moberly
Michael O. Garcia

We certify that we have read this thesis and that in our opinion it is satisfactory in scope and qualify as a thesis for the degree of Master of Science in Geology and Geophysics.

THESIS COMMITTEE

Gordon A. Macdonald
Chairman

Michael O. Garcia

Nahum Mobarry

ABSTRACT

The geology of the upper part of the southwest rift zone of Haleakala was mapped and studied in detail. Late stage alkalic lavas of both the older Kula Formation and the post-erosional Hana Formation are exposed within the study area. Kula lavas are characterized by hawaiites, with subordinate alkalic olivine basalts. Hana lavas are of the same types as those of the Kula Formation, but alkalic olivine basalts predominate and ankaramites are more abundant. Pyroclastic debris covers large areas along, and downwind of the rift. The amount of weathering, which tends to follow climatic variations with changes in elevation, affects the quality and extent of exposures.

Analyses indicate that there is an overlap in chemical trends between the Kula and Hana Formations. Lavas of both formations are enriched in alkalis, whereas Hana lavas are more deficient in silica, and are possibly transitional to the nephelinic suite.

The general excellence of outcrop quality and lack of any major unconformities in the map area, along with petrographic similarities and the overlap of chemical trends, indicate that along the southwest rift zone, there was no appreciable interval of quiescence between the two formations, as apparently occurred on other parts of Haleakala.

TABLE OF CONTENTS

LIST OF TABLES

LIST OF ILLUSTRATIONS

INTRODUCTION

Purpose and Scope

This project was undertaken to map and describe the geology of the upper part of the southwest rift zone of Haleakala Volcano, Maui. There are good exposures of late stage volcanic rocks of both the Kula and Hana Formations within the study area. Stratigraphic and volcanic features were mapped in detail and are described in the report. Rock specimens were collected for laboratory study. Six samples were chemically analyzed and the results are compared with other previously published analyses of late stage rocks from Haleakala.

Location

The Island of Maui, located approximately 100 km southeast of Honolulu, is the second largest island of the Hawaiian Chain. It consists of two volcanoes separated by a narrow isthmus of alluvium, calcareous sand dunes, and shallow marine deposits overlying lava flows of the Kula Formation of Haleakala. The West Maui Volcano is the older of the two. The eastern part of the island is Haleakala Volcano, which rises to a height of over 3,000 m (10,023 ft.) above sea level (Figure 1). It is built along three rift zones that intersect within the summit depression of the volcano, and trend respectively east-northeast, southwest and north-northwest.

The mapped area consists of most of the Kula State Forest Reserve and the Kahikinui State Forest Reserve west of and including Kahua cinder cone. A small section of land that was mapped, which lies between the two forest reserves just east of Polipoli, belongs to Ulupalakua Ranch. The map area is comprised of the northeast portion of U.S. Geological Survey Makena topographic quadrangle map, published in 1954, and the northwest corner of U.S. Geological Survey Lualailua Hills topographic quadrangle map, published in 1957. The total mapped area is bounded on the north by the northern extreme of both quadrangles at latitude N 20°42'30", on the east by a north-trending line at longitude W 156°15'57", on the south by an east-trending line at latitude N 20°40', and on the west by a line extending S 56° W from the intersection of the 6,000 foot contour line and the northern boundary of the map to the southern boundary of the map area. The area is approximately 36 km^2. It extends from an elevation of 1,512 m (4,960 ft.) to an elevation of 2,990 m (9,800 ft.) near the summit.

The lower parts of the mapped area are accessable from Kahului by State Route 37 and the access road to Polipoli State Park. The higher elevations may be reached from the summit of Haleakala within Haleakala National Park. The Park is accessable by State Routes 37, 377, and 378.

Figure 1. Location of map area.

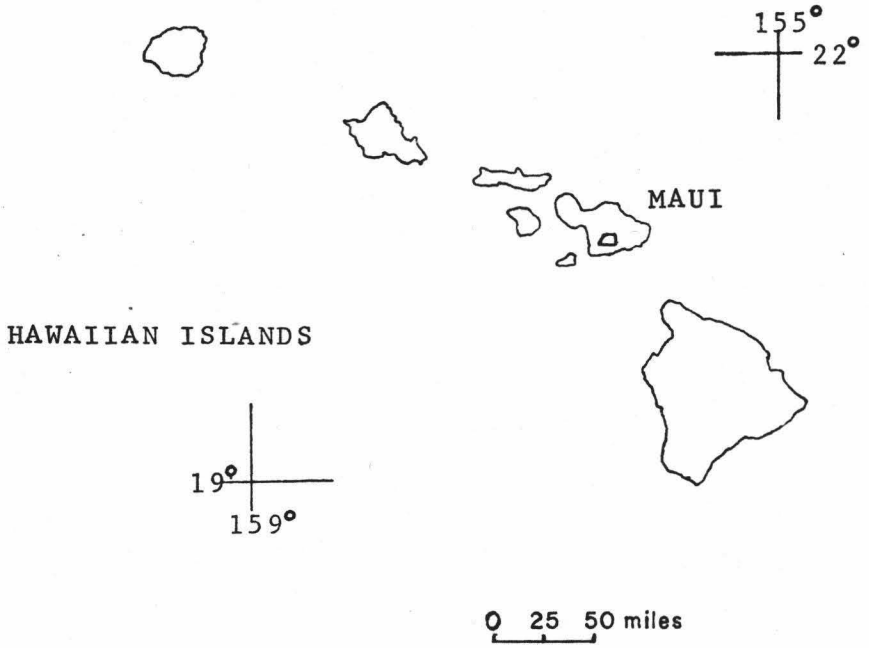
155°
22°
MAUI
HAWAIIAN ISLANDS
19°
159°
0 25 50 miles

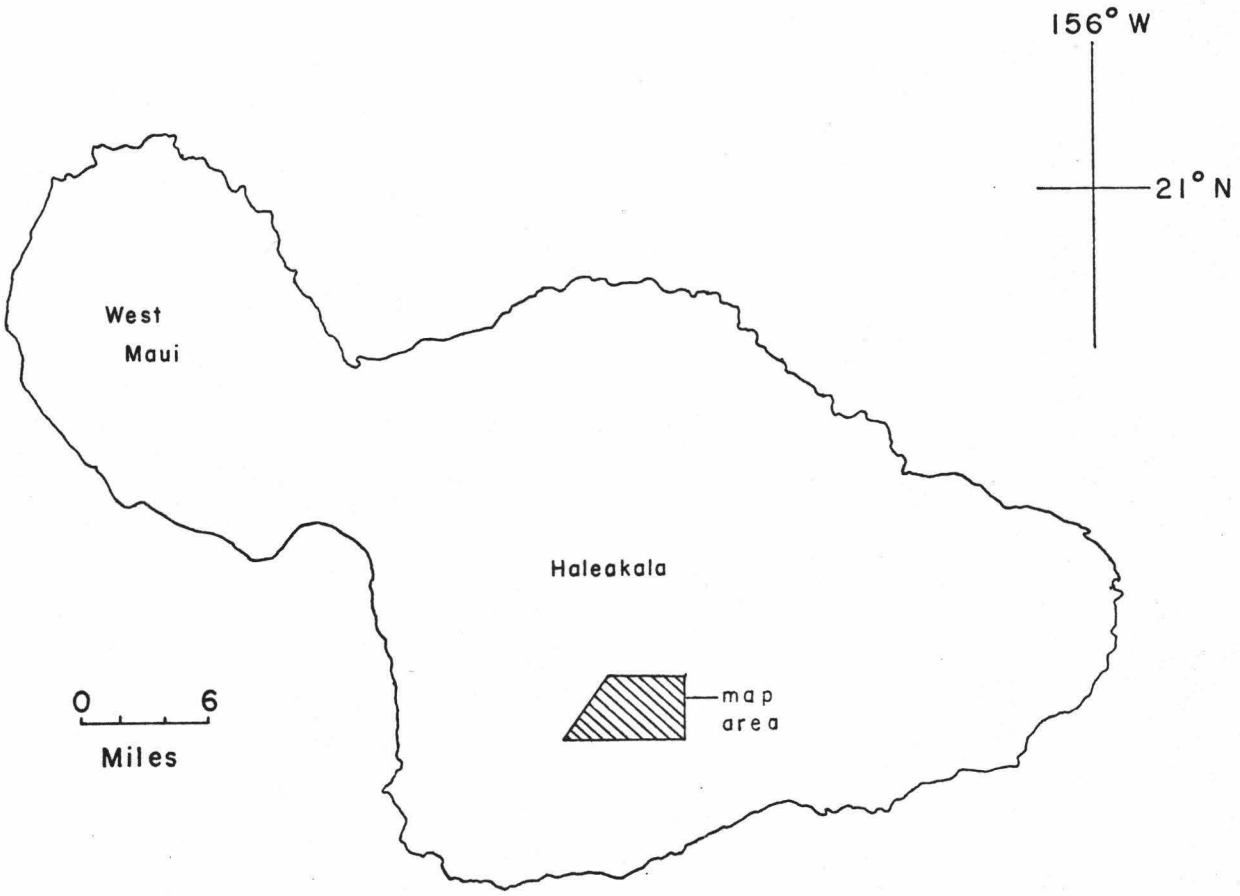
156° W
21° N
West
Maui
Haleakala
map
area
0 6
Miles

Previous Investigations

Most of the early geologic investigations of Maui were descriptive. J. D. Dana, in 1849, described the physiography of portions of Maui based on the notes of Pickering and Drayton, including a sketch by Drayton of Haleakala Crater. E. S. Dana (1889) was the first to describe the petrography of rocks from Maui, and in 1902 Möhle described one specimen of basalt from Haleakala. Cross (1915) studied the chemistry of several rocks from Haleakala and suggested that Haleakala Crater might have an erosional origin. S. Powers (1920) gave analyses of several lavas and compared rocks from different localities. In 1922, Washington and Merwin published a chemical analysis of augite crystals from Haleakala; and in 1928 Washington and Keyes published a study of the petrography and chemistry of late stage lavas of Haleakala. H. A. Powers (1935) compared variations in Haleakala rocks to variations in the rocks of other Hawaiian volcanoes. Stearns and Macdonald (1942) published a study of the geology, petrography and ground-water resources of Maui. They divided the volcanic succession of Haleakala into the Honomanu, Kula, and Hana Volcanic Series. Six new chemical analyses of rocks of the Kula Formation and their petrography were published by Macdonald and Powers in 1946. Reber (1959) attempted to determine the ages of selected late stage lavas of Haleakala by radiocarbon methods. Macdonald and

Katsura (1964) published nearly 150 new chemical analyses for Hawaiian lavas, of which 2 were of late stage Haleakala rocks. McDougall (1964), presented data for potassium-argon age determinations for Hawaiian rocks, including two from the Kula Formation. Oostdam's (1965) new determination of the date of the historic lava flow at La Perouse Bay on the lower southwest rift zone was about 1790. Macdonald and Powers (1968) presented 15 new chemical analyses of rocks of late stage lavas of Haleakala. Keil, Fodor and Bunch (1972) and Fodor, Keil and Bunch (1975) published electron microprobe analyses of feldspars and pyroxenes, respectively, for the lavas of Maui. Brill (1975) mapped in detail and described the rocks of the lower portion of the southwest rift zone of Haleakala.

Methods of Study

Field methods. 73 rock samples were collected in the course of field work during January, February, and May, 1976. The samples were chosen with the view toward thin section study of many and chemical analysis of several of the specimens. Several samples of glassy cinder were collected from a few of the most recent cinder cones. Sampling locations and hand specimen descriptions were noted. Locations were usually determined by compass resection and intersection and by correlation of topographic features with corresponding features on aerial photographs and on the topographic field map. Where vegetation re-

stricted these methods, position was determined by compass bearing and pace. All samples were collected where the location could be accurately determined.

All mapping was done on the Makena and Lualailua Hills quadrangle maps (scale 1:24,000), and occasionally directly on air photographs of approximately the same scale. Contacts were determined by traverse and from those air photographs which showed sharp flow boundaries. All definite contacts were verified by traverse or by eye in the field.

Relative ages of map units were determined by superposition when possible. Due to the wide range of climatic conditions within the mapped area, the use of vegetation cover and degree of weathering to determine relative age can be applied with success only in areas of approximately the same elevation, rock type, and ash cover.

Laboratory methods. Thin sections were made of 56 samples. The petrography of 45 of these was studied in detail and described. Modal percentages were determined by point count and are summarized in Tables I and II. At least 100 points were determined in each thin section. At least 200 points were counted for those samples which were near the borderline between two classifications. Refractive index measurements using oil immersion methods were made on selected minerals which were present in hand specimen but were not found in the corresponding thin section. The

refractive index of glass from a sample of cinder was also measured by immersion methods and used to estimate the silica content of the cinder (George, 1924).

Chemical analyses of 6 selected samples were performed at the University of Manitoba. C.I.P.W. normative minerals were calculated and chemical variation diagrams were plotted using the Graphic Normative Analysis Program of Bowen (1971). These results, along with those for previously analyzed rocks of the Kula and Hana Formations and of average Hawaiian rock types, are summarized in Tables IV and V.

Air photographs were examined stereoscopically and cross-checked with the field data. Some contacts were not apparent in the field, but were observed in the photographs. These were plotted on the base map as approximate contacts.

Acknowledgements

Some thin sectioning, air transportation for myself and shipping of my car to and from Maui, and chemical analyses were paid for by the T. A. Jaggar Volcano Research Fund of the University of Hawaii.

I would like to thank: Harold and Donna Horton for their hospitality while on Maui; Bob Hobdy of the Hawaii Division of Forestry for his help in providing keys to gates within the Kula and Kahikinui Forest Reserves; Kathi

Fulton for typing; Lili Kawaharada for her help in the field and with the graphics; and I am deeply indebted to Harold and Rachel Horton for their support.

PHYSICAL CONDITIONS

Topography

The topography of the upper southwest rift zone is dominated primarily by volcanic features. Cinder cones are most common along the rift, and form a ridge trending S 60° W from the summit area. The increase in elevation along this ridge is approximately 140 m/km (8° slope). Kahua is the only recent large cinder cone within the map area which does not lie on the ridge.

All of the younger Hana cinder cones are associated with lava flows of aa or pahoehoe. The slopes of the cinder cones can be as great as 580 m/km (30°). The older cinder and spatter cones of the Kula formation are generally partially or wholly buried by later lava flows and cinder. Most of the older pyroclastic material occurs along the rift. There are, however, a few small areas of spatter and welded cinder that occur as kipukas isolated within younger flows or cinder away from the rift.

Along the rift, near the summit, are a series of large pit craters. Most of the pit craters lie slightly southeast of the rift. There are small pit craters associated with several of the late stage cinder cones.

The southeastern slope of the rift zone is covered by many well exposed lava flows. The average slope of the surface of these flows is about 300 m/km (17°). The lava is generally fresh and the original clinkery surface of

some flows is still intact. Lava channels occur on many flows. Several lava channels have built levees, by the solidification of overflowing lava along the sides. Some, however, are portions of lava tubes in which the roofs have collapsed while other parts of the tube remains intact. Occasionally, one of the levee-built channels forms a ridge up to 4 or 5 meters above the surrounding lava flow.

Northwest of the rift, the topography is less irregular. Most flows have been buried or partially buried by wind-blown ash and cinder. Stream channels are often incised into the ash and gullying of the slopes has created 1 or 2 fairly large gulches in portions of this area. There are well developed soils at lower elevations. Vegetation is much more abundant on this side of the rift than on the southern side. Alluvium partially fills several closed depressions forming a flat level area within them.

Climate and Drainage

The Hawaiian Islands lie well within the zone of prevailing northeasterly trade winds. The climate varies considerably with elevation and with geographic position on the larger islands such as Maui. Haleakala's large size alters wind flow and the pattern of precipitation. The overall climate ranges from subtropical in the eastern lowlands to temperate in the higher sections of the

mountain.

Temperatures vary seasonally by as much as 10° C on the lower slopes and by about 11° C near the summit (Climate Summary, 1953). The overall difference in temperatures encountered between the lower elevations and the summit area may be as much as 20° C (Climate Summary, 1953; Climates of the States, 1974).

Precipitation generally is greater at the lower elevations. However, "fog-drip" from clouds may contribute a major portion of moisture to areas at higher elevations with no measurable precipitation being recorded (Climates of the States, 1974). During the course of field work in February, 1976, a minor snow storm was encountered near the summit. Rarely, snow extends down to about the 2,200 m (7,200 ft.) level.

During heavy rains, water was observed flowing in intermittent streams. Channel bottoms in these streams are almost always the dense interior portions of aa lava flows. Streams rarely flow farther than several tens of meters before the water disappears into fractures in the stream bed and continues flowing through a permeable layer below the bed. "Springs" were also observed during heavy rains in which water appeared through fractures or joints and continued flowing on the surface. Presumably the mechanisms involved in the disappearing and reappearing streams were the same, depending on the relative head of

the water in each case. In general, however, drainage is not well developed, due to the high porosity and permeability of the lava flows and cinder. Sheet wash probably is as effective as stream flow as an erosive agent. The effects of raindrop impact were observed during heavy rains on the sides of cinder cones, especially where fine ash was exposed.

During the course of field work in the winter months, temperatures below freezing were often encountered during the night at elevations down to 2,300 m (7,500 ft.). Although the rocks and cinder are very permeable, there was a great deal of moisture in the soil at this time of year. Some mornings, long prismatic ice crystals were observed to have "grown" straight out of the soil. These crystals were usually about 3 to 4 cm long, extending from a base of solid ice which included cinder and ash, and branching upward into individual needlelike prisms. Virtually the whole upper surface of loose rock material would be raised as these prisms of ice grew upwards. On one occasion, a flat boulder of approximately 10 kg had been lifted by ice in this manner at least 4 cm. During the day most of the ice melted. Areas of ice within the shadow of bushes, small hills or boulders occasionally would not melt. As the ice prisms melted, they fell over with the result that the soil or rock debris which the ice was supporting tended to move downhill. This form of

solifluction appeared to have as much effect on the movement of loose material downslope as did the heaviest rain.

Vegetation and Outcrop Quality

The amount of rock exposure within the map area varies because of differences in vegetation and degree of weathering caused by climatic changes with changing elevation, and by differences in amount of pyroclastic blanketing.

The outcrop quality on the slope south of the rift is very good. There is little ash cover, and vegetative cover is sparse down to an elevation of about 2,000 m (6,600 ft.). In several cases, contacts can be delineated from differences in vegetative cover. This is especially true in the aerial photographs of this portion of the map area. Below 2,000 m, the amount of grasses and shrubs increase such that the location of some contacts were mapped only approximately.

In general, the northwestern slope shows poor exposures due to heavy ash and cinder blankets and heavy vegetation cover. The prevailing northeast trade winds caused both Kula ash and Hana cinder and ash to be deposited in thick blankets on this side of the rift. Tussock grasses and heath-scrub cover most of the pyroclastic blankets (Vogl, 1971). The Kula Forest Reserve is

planted with a large variety of trees, including cypress, eucalyptus, pine, and redwood. Evergreens are most common and have thrived in the cool, moist climate from an elevation of about 2,200 m (7,200 ft.) down to the lower boundaries of the Kula Forest Reserve and south to the vicinity of Polipoli. Within this area, the older Kula ash is very weathered and has formed soils, in some exposures up to 9 m thick. These soils are usually overlain by Hana ash which often has formed an upper soil layer up to 1 m thick.

Only two Hana lava flows are well exposed on the northwestern side of the rift. As one follows these two flows downhill, the contacts become indistinct until they disappear completely as vegetation and wind blown ash mantle greater portions of the flows. In this area, below an elevation of about 1,900 m (6,200 ft.), the amount of vegetative overgrowth and organic material in the soils formed from both Kula and Hana ashes becomes sufficiently abundant that it was not possible to differentiate between the two.

All mapped areas of alluvium, also partially consisting of colluvium, are covered by alpine tussock grass usually accompanied by scattered ferns and scrubby trees and bushes.

Above 2,300 m (7,550 ft.) the outcrop quality of

both Kula and Hana rocks is excellent due to the very sparse vegetational cover, thin ask cover, lack of moisture and the relatively minor effects of weathering.

STRATIGRAPHY

Regional Stratigraphy

Hawaiian volcanoes pass through several stages characterized by certain rock types or suites. The major shield-building stage is composed of tholeiitic basalts which are slightly oversaturated to slightly undersaturated with silica (Macdonald and Katsura, 1962). This is usually followed by a caldera-filling stage and a post-caldera stage characterized by lavas that are richer in alkalis and poorer in silica than the tholeiites (Macdonald, 1968).

Post-caldera lavas are generally dominated by either mugearites and trachytes, or by hawaiites, ankaramites, and alkalic basalts. Those volcanoes characterized by a cap of mugearites and trachytes are designated the "Kohala type" volcano and those with hawaiite as the predominant lava are termed the "Haleakala type" volcano (Macdonald and Katsura, 1962, 1964). The rock types are not restricted only to one type of volcano. Mugearites are found on Haleakala, whereas hawaiites are also found on Kohala.

The late stage alkalic lavas of the Kohala type volcano form a cap which is separated form the underlying basalts by an erosional unconformity and commonly a bed of ash or soil. In the Haleakala type volcano, the uppermost part of the tholeiitic shield grades upward

into and is interbedded with a series of alkalic basalts, ankaramites and hawaiites (Macdonald and Katsura, 1964). During this stage, eruptions become less frequent and tend to become more explosive, producing more pyroclastic deposits than in the previous stage (Macdonald, 1968).

After a relatively long period of quiescense in which large scale erosional features may be developed, many volcanoes undergo renewed activity. This post-erosional or rejuvenated stage is characterized by lavas which are generally enriched in alkalis and undersaturated with silica. Nepheline often appears in the norm and is abundant in the modes of lavas of some Hawaiian volcanoes (Macdonald, 1968).

The lavas of Haleakala were separated by Stearns and Macdonald (1942) into three volcanic series. Current revision of Hawaiian stratigraphic nomenclature alters the designation of these volcanic series to formations (Macdonald, verbal communication, 1977). The Honomanu Formation of tholeiitic olivine basalt, with lesser amounts of basalt and picrite basalt of the oceanite-type, grades upward, with no real break, into the alkalic rocks of the Kula Formation. Exposures of Honomanu rocks occur only in valleys and sea cliffs along the northern coast.

Kula lavas are predominantly thick, blocky hawaiites, with some alkalic olivine basalts, picrite basalts and

ankaramites, and a very few mugearites (Macdonald and Powers, 1946; Macdonald, 1968). Kula volcanic rocks are separated in most areas from the "post-erosional" lavas of the Hana Formation by a profound erosional unconformity. Locally, however, there may be no evidence of a break in activity.

The Hana lavas are of the same types as those of the Kula Formation, but alkalic olivine basalts predominate. Ankaramites are more abundant, and the hawaiites are in general more mafic and more undersaturated with silica than are their Kula counterparts. Normative nepheline is common in the Hana lavas (Macdonald, 1968).

Kula lavas and pyroclastic cones are exposed along the northwest rift zone and along the higher elevations of the upper southwest rift zone. Large sections of Kula lavas are exposed in the crater walls of the summit depression.

Hana lavas and cones have buried or partially filled many valleys, including the floor of the erosional caldera. They also cover extensive portions of the eastern rift zone and the lower southwest rift zone (Stearns and Macdonald, 1942).

Only one eruption of Haleakala occurred within historic times (Stearns and Macdonald, 1942). A lava flow low on the southwest rift zone formed Cape Kinau near La Perouse Bay in about 1790 (Oostdam, 1965).

Local Stratigraphy

Lavas and tephra of both the Kula and Hana Formations are exposed within the mapped area. There are no exposures of the Honomanu Formation associated with the southwest rift zone. Sample locations are indicated on Figure 3 and are described in Appendix A.

Map units (Plate 1) are, for the most part, comprised of individual lava flows, with associated cinder and spatter cones, cinder and ash blankets, and minor areas of alluvium. In this report, for ease of discussion, map units will be referred to by the appropriate corresponding map symbols used in Plate 1. Figure 2 indicates the relative stratigraphic position of the map units. Within each formation in Figure 2 those units that lie directly above another unit are shown to be younger by superposition. Where superposition was not established, the relative age of map units was estimated by the degree of alteration and weathering and the apparent plant succession. This estimated stratigraphic sequence is shown in Figure 2 by later units lying above, but offset from, older units.

Pyroclastic deposits were not separated stratigraphically except to the extent of assignation to either the Kula Formation or the Hana Formation. Individual cinder cones and consolidated spatter and cinder deposits were mapped when they could be separated locally from other

Figure 2. Correlation of map units. Symbols as shown in Plate 1.

CORRELATION OF MAP UNITS

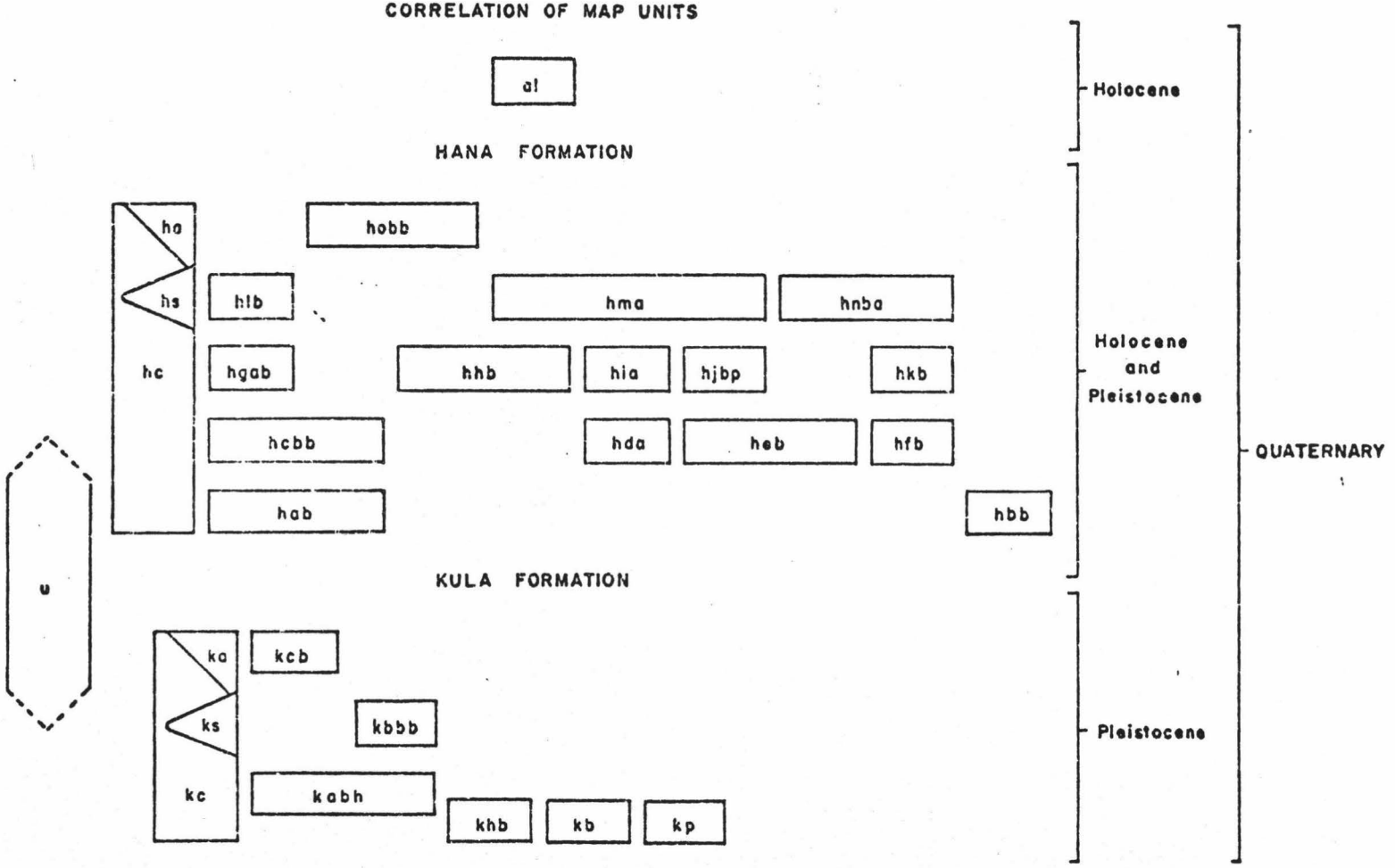

volcanic features. In general, however, the pyroclastics are ubiquitous and the sequence often complicated by early alteration and heavy soil and vegetational cover.

Kula Formation. Three map units appear to be among the oldest rocks exposed on the southwest rift zone. None of these units is separated as to source. The only surface exposure of unit kb large enough to be mapped is a patch of weathered aa at the head of a small gulch about 130 m southeast of Polipoli. Sample P-2 is from the upper vesicular portion of this alkalic olivine basalt flow. In thin section, the sample is fresh in appearance and shows a very well developed flow structure. Included with the kb unit are several other scattered alkalic olivine basalts which were not mapped, however, due to extremely small exposures. Sample P-4 is from a 6 m to 9 m thick section of aa interbedded with red cinder and spatter exposed inside the "Cave Shelter" within the vent of the cinder cone on the southern slope of Polipoli. Samples AR-11 and AR-12 were collected in a vertical roadcut along the major access road to the map area 2.5 km and 2.8 km, respectively, northeast of the junction of the access road and the side road to Polipoli Springs. Both flows are overlain by weathered ash and deep soil up to 9 m thick, which is, in turn, overlain disconformably by a thin layer of younger Hana ash and soil. These beds and the lava flows are parallel to and

Figure 3. Map of sample locations and flows. Patterned areas indicate exposures of the Kula Formation. Underlined sample numbers indicate chemical analysis given in Table V.

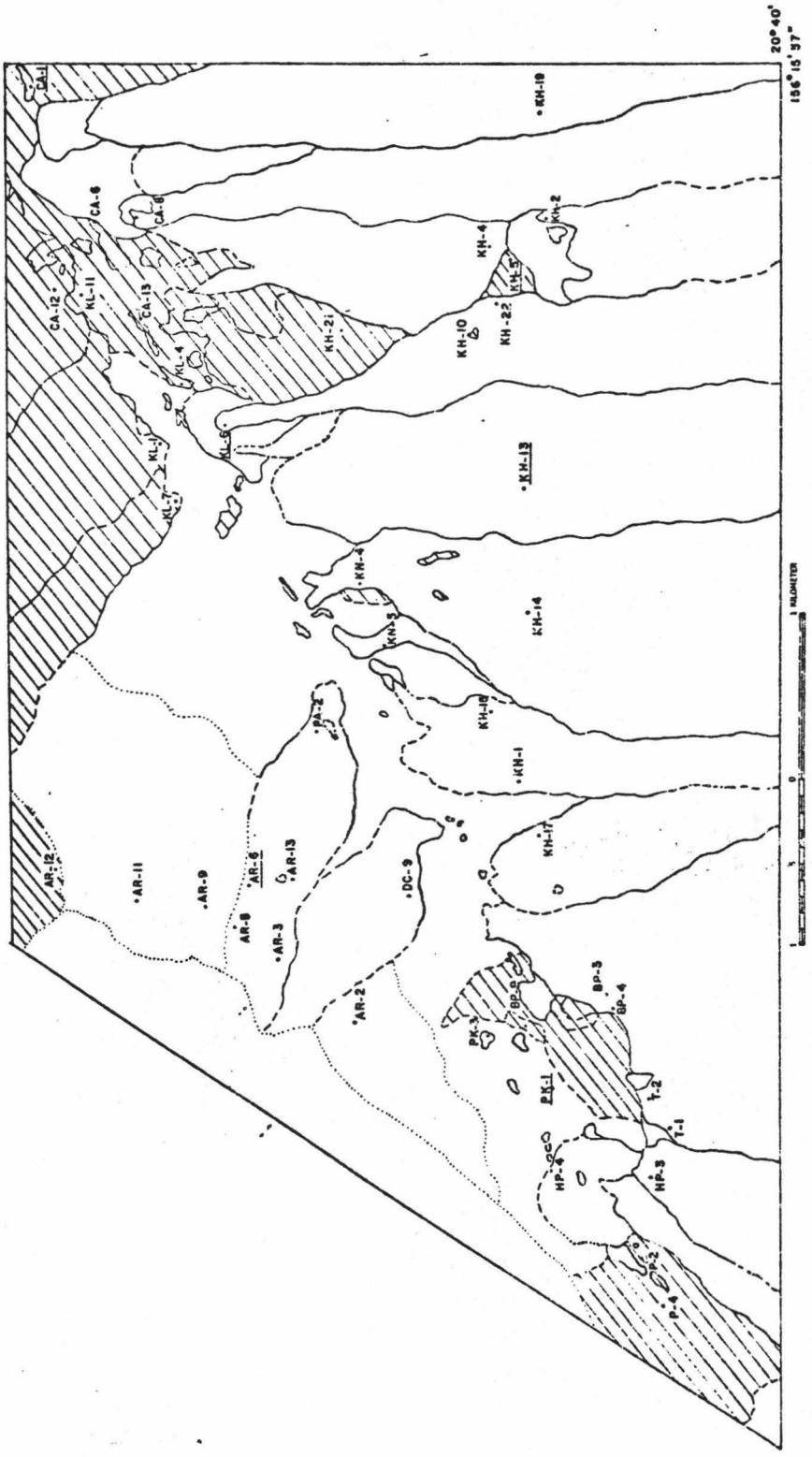
20°40'
156° 13' 37"
CA-1
CA-6
CA-12
KL-11
CA-13
KL-4
KL-6
KL-7
KL-1
KH-21
KH-10
KH-22
KH-4
KH-5
KH-2
KH-19
KH-13
KH-14
KH-4
KH-5
KH-18
KH-1
KH-17
PK-2
AR-12
AR-11
AR-9
AR-8
AR-6
AR-3
AR-13
AR-2
DC-9
BP-5
BP-4
BP-3
PK-3
PK-1
T-2
T-1
HP-4
HP-3
P-3
P-4
1 KILOMETER

follow the present topography, at least locally. Specimen CA-13 is a dense, fine-grained rock which is overlain by a small elongate exposure of welded red cinder and spatter along the rift at an elevation of about 2,800 m (9,200 ft.). In thin section, the rock displays a prominant flow structure with reddish bands of iron oxides and relatively abundant biotite.

Map unit khb is composed of hawaiite lava flows transitional to alkalic olivine basalt. They are scattered near the crest of the ridge along the rift zone. Two small exposures of a very dense, blocky aa occur about 300 m southeast of Puu Keokea. Rare scattered phenocrysts of labradorite up to 9 mm long are apparent in these outcrops. Both exposures flank a large, flat depression, locally known as the "Ball Park", which appears to be the remants of a cinder cone, partially filled with alluvium. The cinder is not welded, although most pyroclastics of the Kula Formation directly along the rift are fairly well consolidated.

The largest area mapped as khb is a triangular shaped section south of the rift and a little more than 1 km southwest of Kahua cone. This portion of the map unit consists of several dense aa flows, each of a uniform thickness of slightly over 1 m, overlying one another. Sample KH-21 was obtained from a small gulch which exposed this section well. The lavas appear to be

almost identical and are difficult to separate laterally.

Above an elevation of approximately 2,700 m (8,800 ft.), four large pit craters were mapped as part of member khb. The lavas exposed within these are Kula hawaiites intercalated with cinder and spatter. However, the minor explosions that formed the craters appear to have occurred during late stage Hana activity (Stearns and Macdonald, 1942). There are numerous blocks with less abundant bombs scattered over the cinder on the upper elevations of the rift. One large shattered block of black glass (sample KL-11), collected from a block-strewn field of predominantly Kula cinder at an elevation of about 2,800 m (9,200 ft.), consists almost entirely of dense black glass and skeletal crystals of olivine. The glass appears to be fresh, but it is uncertain whether the block is an accessory or an essential ejectum (Johnston-Lavis, 1885-86). It was apparently solid at the time of ejection. There are several small isolated outcrops of hawaiite that occur as kipukas in the surrounding pyroclastic cover.

North of Kahua cinder cone is a small triangular outcrop of clinkery picrite basalt. The flow remains as a large kipuka bounded on the northeast and west by later Hana lava flows hab and hobb, and by the Kahua cone on the south.

The stratigraphic positions of map units kb, khb, and kp can not be determined accurately because of the lack of superposition and the overall discontinuity of the isolated exposures of the rocks that are assigned to each unit.

Alkalic olivine basalt, transitional to hawaiite (kabh), forms kipukas of dense aa, alternating with layers of welded cinder, near Kalepeamoa. The same pattern of interbedding of lava with cinder occurs in the khb pit craters previously discussed. The immediate area is covered with black glassy cinder of Hana age. A large aa flow of kabh northwest of the rift extends toward Maui's central valley.

Flows kbbb and kcb both postdate the large kabh flow, as indicated by superposition. Flow kbbb, although not in contact with kcb, appears to be the older of the two because of greater surficial weathering of the surface. Unit kbbb is an alkalic olivine basalt, transitional to alkalic basalt with a total of only 5 percent olivine. The flow is blocky, with areas near the rift covered by wind blown ash and cinder.

Flow kcb is a dark gray alkalic olivine basalt with large poikilitic augite phenocrysts. It overlies flow kabh. The southwest border of the flow is separated from a blanket of Hana cinder by a small intermittent stream which has apparently formed at the boundary of the flow.

Downslope, the contact becomes less distinct due to greater soil development and increased moisture and vegetative cover.

The distribution of pyroclastic rocks is shown in Plate 1. Polipoli and the surrounding areas consist of cinder (kc) and ash (ka), deeply weathered in the upper layers. The cone south of Polipoli, from which sample P-4 was obtained, is composed of red cinder. Considering the extensive soil development within the forest about 20 m away, the volcanic activity that produced this cone must have been among one of the latest Kula events on the rift. There are large exposures of kc along the rift near the summit. Little alteration of the cinder has occurred due to the aridity at the higher elevations. Some areas are strewn with blocks probably ejected during the formation of the pit craters in this area. Ash (ka) and cinder have developed deep soils. Overlying AR-11 is a blanket of ash and soil up to 9 m thick. As discussed above, ks consists of spatter and welded or consolidated cinder. Within the map area, outcrops of ks are invariably weathered to red or red-brown, and occur primarily as kipukas surrounded by younger lavas and tephra. The vents that erupted Kula lavas along the southwest rift zone are, for the most part, buried by later eruptions or have been removed by erosion.

The area mapped as undifferentiated (u) is soil with heavy vegetation and forest cover. It was not possible in the field to determine the source of the soil. It probably was derived from both Kula and Hana ash blankets.

Hana Formation. Lavas of the Hana Formation are better exposed than the earlier Kula lavas which they tend to cover. Superposition of flows is determined more easily.

One of the oldest flows of the Hana Formation is hab, an alkalic olivine basalt lava flow from a very large cinder cone 0.3 km southwest of the CAA Repeater Station near the summit of Haleakala and west of the source cone of flow hlb. The vents for flows hlb and hgab formed cinder cones on the flanks of this larger cone. Flow hlb, a dark gray aa, covers a large portion of hab to the east. Erupted from twin cinder cones, hgab flowed across hab and divided the exposure of hab into two areas. Kahua cinder cone and the recent flow hobb overlie the southern areas of flow hab. A small triangular exposure of picrite basalt of Kula age (kp) was bypassed by hab and left uncovered. Kula cinder and ash have been blown onto portions of the flow near the twin cinder cones. Scrubby bushes and grasses have taken hold and have extensively covered flow hab.

The stratigraphic relationship of unit hbb with other Hana rocks is unknown. Only one small mappable

exposure of this alkalic olivine basalt was observed, a small area of very vesicular pahoehoe in a depression just east of Puu Keakea. The area is covered by fresh cinder from Puu Keokea and has a heavy cover of thick grasses and large scrubby bushes. The source of the lava is unknown. Included with map unit hbb is sample AR-2, an alkalic olivine basalt collected from upslope of the access road through Kula Forest Reserve, about 1.0 km northeast of the junction with the entrance to Polipoli Springs. This flow is overlain and buried by a thin layer of ash and cinder.

Flow hcbb was erupted from Kahua cinder cone. The lava appears to have overflowed the rim and mantled the outer southern side of the cone. The pahoehoe lava flow is a medium gray alkalic olivine basalt, transitional to alkalic basalt. It is overlain laterally by flow hobb on the west and hgab on the east. Below 1,800 m (5,900 ft.) the contacts between these flows and hcbb are recognized with difficulty due to continuous vegetative cover. Sample KH-2 was collected on the southern flank of Kahua. Olivine is wholly or partly altered to iddingsite, possibly because of the proximity of the vent to the sampling site, with accompanying alteration by escaping gases.

An ankaramite lava flow (hda) on the northern slope of the large cone 1.4 km east of Puu Keokea, is one of

the few Hana flows exposed within the map area north of the rift. The flow appears to have been erupted from one or more small spatter cones northeast of the main vent of the large cone. Unit hda is predominantly pahoehoe but locally grades into aa. It is extensively covered by ash downslope. Flow hda is overlain by part of map unit hia on its northern margin. The ash and soil cover and the forestation becomes sufficiently great below 1,900 m (6,200 ft.) that the area is mapped as undifferentiated (u).

An alkalic olivine basalt lava flow (heb) was extruded from the large cinder cone 1.4 km east of Puu Keokea and extends down the southern slope. The flow narrows downslope due to lateral encroachment of overlying units hnba and hjbp. The lava is a dark gray vesicular aa with slight flow structure. The surface is rough with much spinose clinker. A small spatter cone (hs) formed on the surface of flow heb, about 0.4 km south of the main vent.

A dark gray pahoehoe flow of alkalic olivine basalt was erupted from the well developed large cinder cone 0.7 km northeast of Polipoli, and is designated hfb on Plate 1. The surface texture is fairly smooth, especially near the vent, where the characteristic ropy surface of pahoehoe is evident. Flow hfb is overlain by hkb, which appears to be much like hfb but is younger as shown by superposition.

Map unit hgab is an ankaramite, transitional to alkalic olivine basalt. It is a dark gray, moderately rough surfaced, pahoehoe lava flow erupted from the small twin cinder cones 0.9 km southwest of the CAA Repeater Station. Sample CA-8 was collected in a lava channel immediately south of the vent. Sample CA-8a contains a few large xenocrysts of sodic labradorite. Unit hgab flowed across unit hab, as was discussed above, and banked up against and flowed around Kahua cinder cone. Unit hlb postdates hgab, however.

A small cinder cone along the rift about 0.8 km northeast of Kanahau erupted a moderately smooth-surfaced aa flow on the southern side of the rift. Mapped as hhb, it is an alkalic olivine basalt which, by the principal of superposition, is older than units hma and hobb. It is placed stratigraphically above all of the previously discussed units except hgab because of the relative freshness of the surface and small amount of vegetational cover. On the flank of the cinder cone, a small pit crater developed in the flow and may be a secondary vent. There is no evidence that it is a collapsed lava tube.

Map unit hia is composed of several lava flows from Kanahau, which probably were nearly contemporaneous and were erupted from the same vent. The unit consists predominantly of dark gray pahoehoe with minor amounts of aa. Eight samples were collected from the map unit, all

but two of which were ankaramites. Sample AR-8 is from the clinkery portion of an aa, and contains enough olivine phenocrysts to be classified as a picrite basalt, transitional to ankaramite. Sample AR-9 is enriched sufficiently in plagioclase (32 percent in the mode), that it must be classified as an alkalic olivine basalt, transitional to ankaramite. It is overlain by a thin layer of ash. All eight samples appear much the same petrographically (see Petrography), with only minor differences in the relative abundances of phenocrysts and microphenocrysts of olivine, pyroxene and plagioclase. Mineral compositions, as determined optically, are quite similar. There is a short exposure of hia ankaramite on the southern side of the rift which extends about 0.7 km downslope, where it is overlain by flow hma that was erupted from an area toward the northeast on Kanahau. The northern portion of hia is exposed downhill from the road on the western slope of Kanahau. Tracing back toward its source, the flow disappears under the cinder of the cone. A small spatter rampart (hs), about 0.6 km west of the Kanahau benchmark, has been mapped separately. The amount of cinder and ash cover increases downslope, and below an elevation of about 2,200 m (7,200 ft.) the margins of the flow become obscure. Ash blankets the lower portions of the unit and the vegetational cover increases. A large spatter cone is found at an elevation of about

2,100 m (6,900 ft.). The cone appears to be a surface feature of the flow. Unit hia overlies portions of hda. The downhill parts of hia have a heavy ash and vegetational cover which grades into the undifferentiated unit (u).

Unit hjbp is an alkalic olivine basalt flow from the large cinder cone 0.8 km southwest of the benchmark at Kanahau. The cone consists of two vents about 130 m apart. The flow, clinkery pahoehoe and aa, is overlain by unit hma. Near the vents the head of flow hjbp is covered by the cone. Portions of the flow are locally enriched in olivine and approach picrite basalt in mineralogical composition.

The alkalic olivine basalt flow (unit hkb) from a small vent on the south flank of the large cinder cone just east of Polipoli, was very fluid when erupted. The vent appears to be a small pit crater, but is actually a spatter cone buried by its own flow which formed a shallow pond behind and around it and that later collapsed into the vent. The surface was still plastic at the time of collapse, as indicated by sagging of the flow into the opening. The flow moved south-southwest down the rift. Very little lava spilled down the steep slope east of the vent. Flow hkb overlies, but is probably not much older than, unit hfb, as indicated by the degree of weathering, and lack of heavy vegetational cover.

Sample KH-19 was collected from flow hlb, an alkalic olivine basalt, about 0.8 km east of Kahua at the edge of the trail. Flow hlb was erupted from the large cinder cone 0.2 km south of the CAA Repeater Station near the summit. The flow appears to be a thick aa with many lava channels on the irregular surface. It overlies both hab and hgab. It is a fine-grained lava with few phenocrysts.

Unit hma is an ankaramite lava flow from a vent on the northeastern side of Kanahau. Sample KN-4 is from one of the many lava channels on the surface of hma. The flow was erupted south of the rift. The flow lies to the east of a large patch of welded Kula cinder that formed a barrier ridge and apparently caused hma to flow around it. At an elevation of about 2,300 m (7,550 ft.), two kipukas of similar Kula cinder or spatter project through the flow. Unit hma is one of the most recent, overlying hjbp, hia, and hhb.

Unit hnba was erupted from the large cinder cone 1.0 km east of Puu Keokea. The upper portion of the flow near the vent is buried by the cinder cone. The flow is an alkalic olivine basalt transitional to ankaramite. In places it is sufficiently enriched in large augite phenocrysts that locally it may be classified as an ankaramite. Flow hnba, a dark gray aa, spills down a steep slope toward the west, where it is thickened and upheaved. It appears to have banked against another ridge 1.0 km east

of Polipoli, and buckled, forming a large tumulus-like feature about 5 to 6 m high. The flow extends down slope and out of the map area to the south. It directly overlies flow heb to the east and flow hkb to the west.

The youngest flow in the map area is unit hobb, an alkalic olivine basalt, transitional to alkalic basalt. Unit hobb was erupted from a vent 0.3 km south of Kalepeamoa. The flow is pahoehoe with a very fresh, nearly black surface. Rare large xenocysts of andesine-labradorite are present locally within the flow. There is little vegetational cover. Exposed within the flow is a kipuka of Kula spatter (ks) about 0.7 km northwest of Kahua. Pieces of spatter and welded cinder have broken off and have formed the cores of accretionary lava balls which are found downslope of the kipuka.

Hana pyroclastic rocks cover large portions of the map area northwest of the rift zone (Plate 1). Hana cinder (hc) forms cones along the rift except where Kula cinder is exposed as indicated previously. Where they could be separated from the surrounding pyroclastic cover, cinder cones were mapped individually. Differences in colour were also used to help determine relative stratigraphic position with older cones usually being redder than younger cones. Sample HP-4 is a chunk of scoria from the cinder cone 0.3 km southeast of Polipoli Springs. A deep

roadcut shows that the bedding of this cone overlies the cinder from Puu Keokea.

The cinder cover grades into ash (ha) farther downslope on the northwestern side. Due to the small particle size and increased moisture, soil development and vegetational cover is greater at the lower elevations. The areas mapped as ha grade into u (undifferentiated).

Hana spatter (hs) occurs primarily at vents. These vents may be the primary sources of lava flows, and are usually associated with much loose cinder. Spatter may also occur as small secondary cones or ramparts on the surface of flows. The extent of hs is small compared with the other pyroclastic units of the Hana Formation.

Alluvium consists primarily of gravel, sand, and silt generally deposited in closed depressions and small stream channels. Deposits large enough to map occur only in closed depressions. Alluvium is usually covered by tussock grasses.

PETROGRAPHY

Methods

Forty-eight thin sections were examined in detail. In some instances, two or more specimens from different locations within the same flow were compared for textural and mineralogical variations. For purposes of staining or to study a mineral that was observed in hand specimen but not in the original thin section, two thin sections were occasionally made from the same sample. Point count modal analyses for samples from the Kula Formation and Hana Formation are given in Tables I and II, respectively. Due to the small grain size of matrix minerals, almost all thin sections were ground to a thickness of about 10 to 20 microns.

The rocks were classified on the basis of modal amounts and compositions of olivine, pyroxene, and plagioclase as suggested by Macdonald and Katsura (1964). A summary of their classification is as follows:

Alkalic basalt -- contains 30 percent or more total feldspar; less than 5 percent olivine.

Alkalic olivine basalt -- contains 30 percent or more total feldspar; 5 percent or more olivine.

Basanitoid -- contains more than 5 percent normative nepheline, but none in the mode.

Picrite basalt -- contains less than 30 percent total feldspar; abundant olivine phenocrysts.

Ankaramite -- contains less than 30 percent total feldspar; abundant olivine and augite phenocrysts; augite exceeds olivine.

Hawaiite -- average feldspar is andesine; often with basaltic habit; the term "andesite" is employed in older usage.

Plagioclase phenocryst and microphenocryst compositions were determined by variations in extinction angles of combined Carlsbad-albite twins in sections normal to (010) when possible (Tröger, 1971, p. 130). Compositions of groundmass feldspar showing albite twins were determined using the Michel-Lévy statistical method and comparing the results with compositional curves in Heinrich (1965, p. 364). The microlite method (Heinrich, 1965, p. 364) was also used when properly oriented albite twins were not observed, but this method is less accurate than the preceding. In general, the optic axial angle was not useful in determining plagioclase compositions. Albite and Carlsbad twinning are very common, with pericline twinning less so.

Refractive index measurements were made on several feldspar and augite phenocrysts. Where centered interference figures could be found, the optic axial angle was determined by the Kamb or Tobi method, or was estimated from the curvature of the isogyres of a centered optic axis figure (Bloss, 1961). Modal composition and vesi-

cularity were determined by point count. Textural terms follow the usage of Johannsen (1931).

Kula Formation

Hawaiites. Hawaiites of the Kula Formation exposed on the upper southwest rift zone are all transitional to alkalic olivine basalt. They are generally massive, blocky aa lavas. Textures are intergranular to intersertal with glass content ranging from 1 to 4 percent. The glass is pale brown to colourless. Scattered small phenocrysts of olivine up to 3 mm long are present and generally show a small range of 2V of from -88° to -89°. Several grains in specimen BP-9a, however, are slightly zoned with birefringence increasing and -2V decreasing to about 85° near the edge, indicating a slight iron enrichment. Olivine is subhedral to euhedral, often prismatic and slightly skeletal. In sample CA-1, olivine is generally rounded with slight alteration to iddingsite. A few grains show an additional thin rim of olivine around the iddingsite.

Pyroxene phenocrysts are rare with no more than 2 percent in any specimen. Colours range from light dusty brown to dark green brown. Dispersion is usually strong with $v<r$. The pyroxene is augite with an optic angle of 55° to 58°. Refractive indices for an augite phenocryst from sample BP-9b are $\alpha=1.700$, $\beta=1.706$, $\gamma=1.726$. Both

augite and olivine microphenocrysts are often glomerophyric.

Feldspar microphenocrysts are zoned from cores as calcic as bytownite (An_{75}) to rims of medium labradorite. Sample BP-9 contains scattered phenocrysts of plagioclase up to 9 mm long with +2V of about 88° and refractive indices of α= 1.560, β= 1.563 and γ= 1.567. The estimated composition of these phenocrysts based on refractive indices and extinction angles is about An_{62}.

Matrix plagioclase laths are predominantly andesine, but microlites zoned from cores of sodic labradorite to rims of medium to sodic andesine were found. Sample CA-6 contained what appears to be high potassic oligoclase (An_{29}) with small positive axial angle of from 10° to 40° as described by Macdonald (1942). Interstitial alkali feldspar was found in all hawaiites examined except sample KH-21, with sample CA-1 containing up to 3 percent alkali feldspar. Small flakes of biotite, pleochroic from pale yellow-brown to dark red-brown, are usually present interstitially with the alkali feldspar. Opaques appear to be small equant grains of magnetite. Dendritic opaque needles are found in interstitial glass and feldspar in those samples with intersertal textures.

Alkalic olivine basalts. Two specimens of alkalic olivine basalt, transitional to hawaiite, could perhaps have been better discussed with the hawaiites which they

TABLE I. -- Point Count Modal Analysis of Samples of the Kula Formation, Upper Southwest Rift Zone, Haleakala

Sample Number	AR-11	P-2	P-4	BP-9b	KH-5	KH-21
Rock Name	Alkalic Olivine Basalt	Alkalic Olivine Basalt	Alkalic Olivine Basalt	Hawaiite	Picrite Basalt	Hawaiite
Vesicularity	13%	26%	14%	1%	13%	1%
Phenocrysts & Microphenocrysts						
Olivine	17	5	8	5	11	6
Clinopyroxene	7	--	4	tr	9	1
Plagioclase	14	17	7	4	16	19
Magnetite	tr	2	--	tr	2	3
Groundmass						
Olivine	--	5	3	7	3	7
Clinopyroxene	22	22	33	29	22	25
Plagioclase	28	25	25	33	10	26
Alkali Feldspar	--	--	--	1	--	--
Opaques*	9	13	12	17	12	11
Biotite	tr	--	--	tr	--	--
Apatite	--	tr	1	--	--	tr
Iddingsite	tr	tr	1	--	--	--
Iron Oxides**	--	tr	--	--	tr	--
Zeolite	tr	--	--	--	--	--
Glass	3	10	5	2	12	1
Unknown	--	1	1	2	3	1

*Opaques are predominantly Magnetite and Ilmenite.
**Iron Oxides are Hematite, Limonite, Goethite, etc.

TABLE I. (Continued) Point Count Modal Analysis of Samples of the Kula Formation, Upper Southwest Rift Zone, Haleakala

Sample Number	KL-1	KL-4	KL-7	CA-1	CA-6
Rock Name	Alkalic Olivine Basalt	Alkalic Olivine Basalt	Alkalic Olivine Basalt	Hawaiite	Hawaiite
Vesicularity	22%	5%	12%	5%	11%
Phenocrysts & Microphenocrysts					
Olivine	3	6	6	5	8
Clinopyroxene	--	--	12	2	2
Plagioclase	30	4	22	17	23
Magnetite	5	1	1	tr	3
Groundmass					
Olivine	7	4	--	7	3
Clinopyroxene	18	27	24	24	16
Plagioclase	17	38	16	30	20
Alkali Feldspar	--	1	--	3	tr
Opaques*	12	14	10	13	16
Biotite	--	tr	--	tr	--
Apatite	tr	1	tr	--	1
Iddingsite	--	1	1	--	--
Iron Oxides**	1	--	--	--	2
Zeolite	--	tr	1	--	2
Glass	7	1	5	2	4
Unknown	--	2	2	1	--

*Opaques are predominantly Magnetite and Ilmenite.
**Iron Oxides are Hematite, Limonite, Goethite, etc.

TABLE I. (Continued) Point Count Modal Analysis of Samples of the Kula Formation, Upper Southwest Rift Zone, Haleakala

Sample Number	CA-12	CA-13
Rock Name	Alkalic Olivine Basalt	Alkalic Olivine Basalt
Vesicularity	27%	3%
Phenocrysts & Microphenocrysts		
Olivine	4	6
Clinopyroxene	12	--
Plagioclase	17	--
Magnetite	2	1
Groundmass		
Olivine	1	6
Clinopyroxene	25	17
Plagioclase	17	37
Alkali Feldspar	--	2
Opaques*	12	13
Biotite	--	6
Apatite	--	--
Iddingsite	--	3
Iron Oxides**	2	5
Zeolite	5	--
Glass	2	2
Unknown	1	2

*Opaques are predominantly Magnetite and Ilmenite.
**Iron Oxides are Hematite, Limonite, Goethite, etc.

petrographically resemble. Samples KL-1 and KL-4 are, however, classified as alkalic olivine basalts based on an average plagioclase composition of labradorite.

Sample KL-1 has an intersertal texture with 7 percent glass, moderate vesicularity, and shows flow structure in thin section. Olivine microphenocrysts have $-2V = 89^{o}$. Many olivine grains are skeletal and filled with glass or interstitial feldspar, and commonly have rims of dusty opaque grains. There are inclusions of bits of cinder containing small grains of olivine, pyroxene and plagioclase and much fine granular iron ore. One phenocryst of plagioclase in the cinder is bytownite with a composition of about An_{80} and β refractive index of about 1.56. Most feldspar phenocrysts and microphenocrysts in KL-1 are labradorite, but very small microlites in the groundmass are as sodic as andesine (An_{43}).

Sample KL-4 has an intergranular texture and is fairly dense with only 5 percent vesicles. Olivine microphenocrysts are subhedral to anhedral and rounded with $-2V = 88^{o}$. Some have a thin rim of iddingsite. Pyroxene is found only in the groundmass as small equant grains. There is a trace of redbrown biotite and 1 percent interstitial alkali feldspar. Several grains of alkali feldspar project into vesicles and show fairly well developed cleavage parallel to the fast ray. The refractive index is below balsam. A trace of zeolite is

present as vesicle lining. Magnetite is generally amoeboid as microphenocrysts and forms small equant grains in the groundmass. Plagioclase ranges from large microphenocrysts of calcic labradorite (An_{69}) to microlites of sodic labraderite (An_{52}).

Other Kula alkalic olivine basalts are generally intersertal with only one specimen collected that was totally intergranular (CA-13). Several samples show slight to pronounced flow structure. Olivine phenocrysts up to 1.7 mm long range from euhedral to anhedral and deeply embayed, even within the same thin section. In those samples with much glass, olivine is commonly skeletal and filled with brown glass. Much olivine is rimmed with iddingsite. Iron oxides and zeolites are commonly present, especially within vesicles. Sample AR-12 has small clumps of glomerophyric olivine grains which appear to be fractured and strained, as indicated by a slightly undulatory extinction. They are occasionally enclosed by slightly pink pyroxene microphenocrysts.

Pyroxene phenocrysts and microphenocrysts range from large euhedral twins to plucked and rounded grains. They are usually zoned, often showing an hourglass structure. The largest grains are often poikilitic with augen-like inclusions of glass or minerals of groundmass texture and composition. In several specimens pyroxenes are often glomerophyric. All pyroxene phenocrysts are augite with +2V usually from 55-58°, but ranging up to 65° in one

specimen. Dispersion is v<r, moderate to strong. Colours range from light brown to slightly pleochroic purplish edges which may be due to increased titanium concentrations. Matrix pyroxene is also augite or sub-calcic augite with +2V down to 35°.

Plagioclase laths range in composition from micro-phenocrysts of sodic bytownite with 2V near 90° to interstitial groundmass labradorite microlites with variable 2V of between 90° and +50°. Glass is usually cloudy brown, but colourless glass was also noted. Late crystallizing interstitial feldspar and interstitial glass often contain dendritic growths of opaques and feathery skeletal crystals which are probably pyroxenes, based on similar morphologics observed in submarine basalts (Bryan, 1972). Several samples of alkalic olivine basalt have vesicles lined with zeolites. Others have vesicle and fracture fillings of ash composed of fresh glass shards.

Sample CA-13 is notable in that it contains up to 6 percent red-brown biotite -- more than any other sample studied from the southwest rift zone. In hand specimen, the rock is a dense, slightly banded lava. The texture is intergranular with a prominant flow structure. The bands consist of small fractures with iron oxide filling and concentrations of biotite, iddingsite-rimmed olivine, and iron oxide stains. Indistinct bands of vesicles parallel and intermingle with the more visible red bands.

This suggests that the banding may be due to late stage volatile transfer along flow planes.

Picrite basalt. Only one specimen of picrite basalt was collected from the Kula Formation within the map area. The texture is intersertal with 12 percent dark brown glass in an extremely fine grained matrix with an average grain size of less than 0.008 mm. Microlites of plagioclase have the composition of calcic andesine. Several small twinned euhedral microphenocrysts of pyroxene yield +2V's near 40° and are probably sub-calcic augite.

Several large plagioclase microphenocrysts are zoned from medium bytownite cores to rims of medium labradorite. Smaller microphenocrysts are as sodic as An_{52}. Feldspar laths are commonly slightly skeletal, showing a swallow-tailed form.

Olivine phenocrysts and microphenocrysts are also commonly slightly skeletal and tend to include small blebs or square grains of opaques. The olivine has a $-2V = 88°$.

Augite phenocrysts are usually subhedral and somewhat poikilitic, with a $+2V = 58°$ and $\gamma\Lambda(110) = 29°$. Microphenocrysts tend to be more euhedral with +2V ranging from 45° to 55°. Pyroxenes often show paired twinning.

Hana Formation

Alkalic olivine basalts. All samples of alkalic olivine basalt collected from the Hana Formation are porphyritic or microporphyritic. Phenocrysts and microphenocrysts of olivine and pyroxene are abundant, except for two map units in which the total amount of olivine drops to an average of about 6 percent. Olivine phenocrysts have 2V very near 90°. They are rounded and embayed to euhedral. Often the smaller grains are more anhedral and are equant to prismatic. Occasional small glomerocrysts of olivine are present. Olivines of sample KH-19 are subhedral microphenocrysts, which are unusual in that several grains show a slight dispersion with r<v. Although 2V ranges from -88° to +87° from grain to grain within the thin section, zoning is not apparent within single grains.

Phenocrystic pyroxene is augite, with measured axial angles of between +50° and +60°. Dispersion is from weak to strong v<r. Pyroxene phenocrysts are subhedral to euhedral, often with a few inclusions of interstitial brown glass in areas that are slightly embayed. Colours range from pale brown to greenish brown with several grains that are zoned to slightly pleochroic purplish brown rims. Concentric and hourglass zoning are quite common.

TABLE II. -- Point Count Modal Analysis of Samples of Hana Formation, Upper Southwest Rift Zone, Haleakala

Sample Number	AR-2	AR-3	AR-6	AR-8	AR-9	AR-13
Rock Name	Alkalic Olivine Basalt	Ankaramite	Ankaramite	Picrite Basalt	Alkalic Olivine Basalt	Ankaramite
Vesicularity	12%	10%	13%	32%	11%	9%
Phenocrysts & Microphenocrysts						
Olivine	7	13	12	20	9	10
Clinopyroxene	11	26	28	20	16	24
Plagioclase	22	9	8	11	14	11
Magnetite	1	1	2	1	tr	1
Groundmass						
Olivine	tr	tr	1	tr	3	tr
Clinopyroxene	30	22	21	22	24	19
Plagioclase	12	12	11	13	18	16
Alkali Feldspar	--	--	--	--	--	--
Opaques*	11	11	9	7	12	11
Biotite	--	--	--	--	--	tr
Apatite	--	tr	tr	--	tr	--
Iddingsite	--	--	--	--	--	--
Iron Oxides**	--	--	1	tr	2	--
Zeolite	--	--	--	--	--	tr
Glass	5	5	7	5	1	8
Unknown	1	1	--	1	1	--

*Opaques are predominantly Magnetite and Ilmenite.
**Iron Oxides are Hematite, Limonite, Goethite, etc.

TABLE II. (Continued) Point Count Modal Analysis of Samples of the Hana Formation, Upper Southwest Rift Zone, Haleakala

Sample Number	HP-3	T-1a	T-2	PK-3	BP-3	DC-9
Rock Name	Alkalic Olivine Basalt	Ankaramite	Ankaramite	Alkalic Olivine Basalt	Alkalic Olivine Basalt	Ankaramite
Vesicularity	31%	6%	9%	58%	13%	13%
Phenocrysts & Microphenocrysts						
Olivine	4	11	12	9	7	5
Clinopyroxene	tr	29	24	2	15	18
Plagioclase	13	21	19	15	20	20
Magnetite	1	7	3	1	2	3
Groundmass						
Olivine	4	2	--	4	2	2
Clinopyroxene	16	13	13	26	20	25
Plagioclase	28	8	10	21	12	8
Alkali Feldspar	--	--	--	--	--	tr
Opaques*	13	8	7	13	9	6
Biotite	--	tr	--	--	--	--
Apatite	1	tr	tr	--	tr	--
Iddingsite	--	--	--	--	--	--
Iron Oxides**	1	--	--	tr	--	--
Zeolite	--	--	--	--	--	--
Glass	18	1	11	8	13	12
Unknown	1	--	1	1	--	1

*Opaques are predominantly Magnetite and Ilmenite.
**Iron Oxides are Hematite, Limonite, Goethite, etc.

TABLE II. (Continued) Point Count Modal Analysis of Samples of the Hana Formation, Upper Southwest Rift Zone, Haleakala

Sample Number	KH-2	KH-4	KH-10	KH-13	KH-14	KH-16
Rock Name	Alkalic Olivine Basalt	Alkalic Olivine Basalt	Alkalic Olivine Basalt	Alkalic Olivine Basalt	Ankaramite	Alkalic Olivine Basalt
Vesicularity	12%	4%	25%	13%	18%	18%
Phenocrysts & Microphenocrysts						
Olivine	3	7	7	8	9	9
Clinopyroxene	5	tr	10	10	20	9
Plagioclase	12	11	16	18	15	19
Magnetite	3	1	1	1	1	2
Groundmass						
Olivine	3	2	tr	1	tr	3
Clinopyroxene	24	27	25	25	24	24
Plagioclase	25	24	21	19	12	13
Alkali Feldspar	--	--	--	--	--	--
Opaques*	17	19	11	13	10	14
Biotite	--	--	--	--	--	--
Apatite	1	--	--	--	--	tr
Iddingsite	2	--	--	--	tr	--
Iron Oxides**	--	tr	--	tr	--	1
Zeolite	--	tr	tr	--	--	--
Glass	2	7	8	4	8	3
Unknown	3	2	1	1	1	3

*Opaques are predominantly Magnetite and Ilmenite.
**Iron Oxides are Hematite, Limonite, Goethite, etc.

TABLE II. (Continued) Point Count Modal Analysis of Samples of the Hana Formation, Upper Southwest Rift Zone, Haleakala

Sample Number	KH-17	KH-19	KH-22	PA-2	KN-5
Rock Name	Alkalic Olivine Basalt	Alkalic Olivine Basalt	Alkalic Olivine Basalt	Ankaramite	Ankaramite
Vesicularity	28%	10%	5%	31%	5%
Phenocrysts & Microphenocrysts					
Olivine	4	6	6	6	7
Clinopyroxene	10	1	9	18	15
Plagioclase	21	13	17	7	13
Magnetite	tr	1	--	1	1
Groundmass					
Olivine	4	6	--	3	2
Clinopyroxene	17	30	29	22	26
Plagioclase	16	20	23	20	15
Alkali Feldspar	--	--	tr	--	--
Opaques*	15	14	12	11	11
Biotite	--	--	--	--	--
Apatite	1	tr	tr	tr	tr
Iddingsite	--	--	--	--	--
Iron Oxides**	tr	1	1	1	2
Zeolite	tr	2	1***	1	--
Glass	10	5	2	10	8
Unknown	2	1	--	--	--

*Opaques are predominantly Magnetite and Ilmenite.
**Iron Oxides are Hematite, Limonite, Goethite, etc.
***Includes calcite in vesicles.

TABLE II. (Continued) Point Count Modal Analysis of Samples of the Hana Formation, Upper Southwest Rift Zone, Haleakala

Sample Number	KL-6	CA-8b
Rock Name	Alkalic Olivine Basalt	Ankaramite
Vesicularity	20%	14%
Phenocrysts & Microphenocrysts		
Olivine	4	9
Clinopyroxene	11	17
Plagioclase	16	13
Magnetite	tr	1
Groundmass		
Olivine	1	2
Clinopyroxene	32	25
Plagioclase	23	16
Alkali Feldspar	--	--
Opaques*	8	7
Biotite	--	--
Apatite	--	--
Iddingsite	--	--
Iron Oxides**	--	tr
Zeolite	1	--
Glass	3	9
Unknown	1	1

*Opaques are predominantly Magnetite and Ilmenite.
**Iron Oxides are Hematite, Limonite, Goethite, etc.

Groundmass textures range from intergranular to intersertal, with areas within a few samples locally having a hyaloophitic texture. These areas appear to be due to inclusion of cinder or scoria resulting in a concentration of vesicles and glass within the lava. Intersertal textures are most common with glass contents ranging from 4 to 18 percent. Small acicular needles of apatite are commonly included in feldspar laths, but may be absent. Interstitial glass is usually cloudy dark brown and occasionally contains needles of pyroxene and dendritic opaques. Magnetite microphenocrysts are often skeletal and amoeboid. Sample HP-3 is quite vesicular (31 percent). It contains abundant glass (18 percent) and shows what appears to be quench texture around the vesicles, with the glass containing skeletal dendritic magnetite, and feathery and needle-like pyroxene.

Feldspar compositions in the alkalic olivine basalts range from microphenocrysts with cores of medium bytownite to a few groundmass microlites of medium andesine. Optic axial angles are variable, ranging inconsistantly with composition from about -80° to $+60^{\circ}$. The average plagioclase composition is medium to calcic labradorite. Andesine is rare. Alkali feldspar was found only in sample KH-22 in trace amount.

Two lava flows on the southern side of the rift (unit hcbb and hobb) are transitional to alkalic basalt, with between 5 to 7 percent total olivine. Sample KH-2

is from Kahua cone, and has an intergranular to slightly intersertal texture. Small olivine phenocrysts and microphenocrysts have distinct rims of iddingsite, which occasionally appear to be pleochroic from orange to red-brown. Light brown augite has a $+2V = 58^{o}$ and commonly shows hourglass zoning. Both olivine and augite often occur as glomerocrysts. Plagioclase microphenocrysts are normally zoned from calcic to sodic labrodorite with $+2V = 86^{o}$. Groundmass feldspar is sodic labradorite. Opaques are distinctly bimodal in grain size, with subhedral to euhedral equant microphenocrysts up to about 0.4 mm and abundant granular iron ore in the groundmass.

Four thin sections of three different samples taken from flow hobb were studied in detail. Groundmass textures are intersertal, except for sample KH-22, which is from a more dense portion of the flow and in which the texture is intergranular. Groundmass plagioclase composition is medium labradorite. Microphenocrysts are calcic to medium labradorite with 2V of from $+85^{o}$ to -85^{o}. There are a few scattered xenocrysts of andesine-labradorite up to 10 mm long. The β refractive index is about 1.558 with $+2V = 85^{o}$. The xenocrysts are rounded and have a corona of plagioclase apparently of groundmass feldspar composition. The labradorite mantle is about 0.08 mm thick and shows a higher birefringence and slightly higher refractive index. It is crystallographically

continuous but optically discontinuous with respect to the xenocrystic feldspar. Small elongate blebs of glass and a few opaques, aligned with the (010) direction, form a thin layer between the xenocryst and the mantling feldspar. Small equant grains of pyroxene are included within the rim.

Olivine phenocrysts range from euhedral to anhedral and embayed. A few microphenocrysts have rims of dusty magnetite, expecially where grains are near vesicles. A few grains appear to be very slightly normally zoned. One olivine phenocryst from sample KL-6 has an inner rounded core mantled by olivine of approximately the same composition forming a subhedral equant grain. 2V was not determined for this grain due to inappropriate orientation, but the birefringence is constant throughout the phenocryst and comparable to other grains of similar orientation.

Pyroxenes range from microphenocrysts of subcalcic augite with +2V = 40-45°, to phenocrysts of brown or green-brown augite with +2V up to about 60°. Microphenocrysts are often slightly glomerophyric and may even be cumulophyric with olivine microphenocrysts. Phenocrysts of pyroxene are often rounded, and show slight to moderate concentric zoning. Several phenocrysts have optically distinct cores which are mantled by a rim of augite with a small +2V of about 50°. These pyroxenes, the large

andesine crystal and the mantled olivine phenocrysts are probably xenocrystic, and may be present due to inclusion of an older lava, with remelting of all but the largest phenocrysts. An alternative suggesting is that these xenocrysts, especially the feldspar, may be present due to mixing of magmas with remelting or partial remelting of minerals that normally crystallize at lower temperatures (Macdonald, 1965).

Calcite was found as a lining within some vesicles in sample KH-22. This is the only specimen within the map area in which the presence of calcite was definitely established.

Two units of alkalic olivine basalt are transitional to either picrite basalt or ankaramite depending on relative concentrations of olivine and pyroxene. Unit hnba can be locally called ankaramite due to increased amounts of large augite phenocrysts. Olivine phenocrysts are euhedral to anhedral and somewhat embayed. 2V ranges from -88^{o} to 90^{o}. Pyroxene phenocrysts up to 4 mm across can be euhedral to anhedral and embayed within the same thin section. Occasionally, a pyroxene phenocryst will have inclusions of granular opaques and feldspar laths just within and parallel to the rim of the grain. Axial angles range from about $+52^{o}$ to $+62^{o}$. One grain showed an extinction of $\gamma \wedge c = 41^{o}$. Most pyroxene phenocrysts are light brown with a slight pink or purplish tinge. Con-

centrically zoned phenocrysts are often pleochroic, expecially near the rim. Sample T-1a has phenocrysts in which α = light brown, $\beta = \gamma$ = slightly purplish brown. Matrix pyroxenes are usually anhedral and equant. Sample T-2, however, has scattered patches of radial clusters of prismatic pyroxene grains that grossly resemble spherulites. These radiating pyroxene clusters are associated with interstitial dark brown glass.

Groundmass textures are mostly intersertal, with sample T-1a having an intergranular texture. Small prisms or needles of apatite are found in all samples. Plagioclase compositions range from calcic labradorite microphenocrysts to sodic labradorite microlites. Calcic andesine microlites are present in the groundmass of sample BP-3.

Ankaramites. All ankaramites, and one picrite basalt transitional to ankaramite, have intersertal textures with between 5 to 12 percent interstitial dark brown glass. Total feldspar content is less than 30 percent. Compositional range for feldspars of the Hana ankaramites is from microphenocrysts of sodic bytownite to interstitial microlites of sodic labradorite. 2V ranges from -80^{o} to $+85^{o}$. Sample CA-8 includes a few large xenocrysts of sodic labradorite up to 2 cm long. Refractive indices are $\alpha = 1.554$, $\beta = 1.558$, $\gamma = 1.562$. An encircling corona of more calcic plagioclase was

noted, but no optical measurements were obtained. Refractive indices appear to be slightly higher and birefringene is definitely greater for the mantling feldspar. Sample DC-9 has a trace of interstitial alkali feldspar. Iron ore is abundant and often seriate from microphenocrysts of square skeletal grains of magnetite to very small equant grains and needles of either magnetite or ilmenite. These opaque needles are commonly found in the dark brown interstitial glass.

Olivine phenocrysts up to 7 mm long are anhedral to euhedral. Most of them tend to be subhedral with slight to moderate resorption and embayment. 2V extends from -86° to +88°, with most near -88° to -89°. Sample CA-8b contains one grain of olivine that consists of what appears to be a poikilitic center surrounded by a solid rim forming an euhedral crystal. The rim has a slightly higher birefringence than the core, but there is no apparent difference in axial angles.

Phenocrysts of pyroxene are anhedral and rounded to euhedral. Most are slightly poikilitic often with inclusions of either plagioclase microphenocrysts parallel to and near the edges of the grains, or patches of interstitial brown glass, iron ore, apatite and feldspar microlites. +2V is between 54° and 63°. Concentric zoning is common, but hourglass zoning in phenocrysts and martini-glass zoning (Bryan, 1972) in microphenocrysts

were noted. Pyroxene is usually brown to greenish brown, but several samples have pale purplish rims indicating probable titanium enrichment. Pyroxene phenocrysts reach up to 7 mm across. Dispersion is usually v<r, strong, but r<v, weak was observed in grains in the same slide.

Pyroclastic rocks. Pyroclastic rocks are common to both the Kula and Hana formations. Sample KL-11 is a glass block that was ejected from the pit craters near the summit of Haleakala. It is uncertain which formation it comes from. It consists of dark brown, almost black, slightly vesicular glass with inclusions of magnetite microphenocrysts and skeletal olivine and extremely rare microlites of feldspar. Skeletal olivine crystals range in form from a lantern-like form to a doublt swallow-tailed appearance, to hollow euhedral grains. It is estimated that at least 90 percent of the olivine crystals in KL-11 show skeletal forms. Bryan (1972) suggests that the development of skeletal forms is due to rapid crystal growth combined with low diffusion rates in the liquid.

A sample of fresh cinder from the Hana Formation (PK-1) was studied optically. It consists essentially of dark brown glass of refractive index of about 1.621. Comparing this value to the curve relating to silica content and refractive indices by George (1924), gives an approximate silica content for the cinder of about 46

percent. The silica content as determined by chemical analysis (see Table V) is near 42.5 percent.

CHEMISTRY

Chemical Analyses

Six samples collected during the course of study were chemically analyzed. The results, along with calculated C.I.P.W. norms, are shown in Table V. Chemical analyses of other late stage lavas of Haleakala and their norms are also presented in Table V.

On all chemical variation diagrams (Figures 4-15), are plotted compositions of selected average Hawaiian lavas of the alkalic and nephelinic suites (Table IV), and the late stage lavas of Haleakala Volcano. Figures 6-15 also include plots of 6 pyroxenes from Haleakala. Sample numbers, plotting symbols, rock type and sources of data are given in Table III.

The six analyzed samples were chosen to represent most of the major rock types exposed on the upper southwest rift zone. Sample CA-1, from map unit khb, is a Kula hawaiite, transitional to alkalic olivine basalt. KH-5 is a picrite basalt (map unit kp), also from the Kula Formation. Samples from the Hana Formation include an ankaramite (AR-6) mapped with unit hia; sample KH-13, an alkalic olivine basalt from unit hhb; KL-6, an alkalic olivine basalt, transitional to alkalic basalt, from the youngest flow in the map area (hobb); and PK-1, a sample of fresh glassy cinder. Detailed locality descriptions are given in Table I.

TABLE III -- Summary of Plotting Symbols, Rock or Mineral Types, Formations, and Published Chemical Analyses Sources

Sample Number	Plotting Symbol	Rock or Mineral Type	Formation	Source of Chemistry
CA-1	1	Hawaiite	Kula	this paper
KH-5	2	Picrite Basalt	"	"
AR-6	3	Ankaramite	Hana	"
KH-13	4	Alkalic Olivine Basalt	"	"
KL-6	5	Alkalic Olivine Basalt	"	"
PK-1	6	Cinder	"	"
C-129	X	Basanitoid	"	(Macdonald and Powers, 1968)
C-136	X	Basanitoid	"	"
C-138	X	Basanitoid	"	"
C-139	X	Basanitoid	"	"
C-142	X	Basanitoid	"	"
C-148	X	Basanitoid	"	"
C-127	0	Hawaiite	Kula	(Macdonald and Katsura, 1964)
46PB1	0	Picrite Basalt	"	(Macdonald and Powers, 1946)
46A2	0	Andesite	"	"
46A3	0	Andesite	"	"
46A4	0	Andesite	"	"
46A5	0	Andesite	"	"
460A6	0	Oligoclase Andesite	"	"
C-147	0	Hawaiite	"	(Macdonald and Powers, 1968)

TABLE III (Continued) Summary of Plotting Symbols, Rock or Mineral Types, Formations, and Published Chemical Analyses Sources

Sample Number	Plotting Symbol	Rock or Mineral Type	Formation	Source of Chemistry
C-156	0	Hawaiite	"	"
C-135	0	Basanitoid	"	"
C-137	0	Hawaiite	"	"
C-140	0	Alkalic Olivine Basalt	"	"
C-141	0	Mugearite	"	"
C-143	0	Hawaiite	"	"
C-144	0	Hawaiite	"	"
C-145	0	Hawaiite	"	"
C-146	0	Hawaiite	"	"
Aug	+	Augite	"	(Washington and Merwin, 1922)
C137G	+	Clinopyroxene	"	(Fodor, Keil, and Bunch, 1975)
C141G	+	Clinopyroxene	"	"
C142G	+	Clinopyroxene	Hana	"
C139G	+	Clinopyroxene	"	"
C148G	+	Clinopyroxene	"	"
AVTRA	T	Trachyte	*	(Macdonald, 1968)
AVMUG	M	Mugearite	*	"
AVHAW	H	Hawaiite	*	"
AVAOB	B	Alkalic Olivine Basalt	*	"
AVANK	A	Ankaramite	*	"

TABLE III (Continued) Summary of Plotting Symbols, Rock or Mineral Types, Formations, and Published Chemical Analyses Sources

Sample Number	Plotting Symbol	Rock or Mineral Type	Formation	Source of Chemistry
BTOID	D	Basanitoid	*	"
BSITE	E	Basanite	*	"
AVNEF	N	Nephelinite	*	"

*Based on average chemical compositions of the various types of Hawaiian rocks.

The analysis was done by a combination of x-ray flourescence and atomic absorption spectrometry and colorimetry at the University of Manitoba. The results are comparable to previously published data for similar rocks.

Discussion of Analyses

The late stage lavas of Hawaiian volcanoes are notably richer in alkalis and generally poorer in silica than the tholeiitic lavas, and plot in separate regions on a graph of alkalis against silica (Macdonald and Katsura, 1964). It can be seen in Figure 4 that all of the late stage lavas of Haleakala plot in the alkalic field, above the line separating the two regions.

The lavas of the Kula Formation and the post-erosional lavas of the Hana Formation plot in distinctly different regions in most of the variation diagrams. There is overlap between the two formations in all diagrams.

Appendix B consists of MgO variation diagrams (Figures 8-15). An approximately linear variation with respect to MgO is present within the region for each formation. Two exceptions are the plots with P_2O_5 and TiO_2 in figures 12 and 13, respectively. Phosphorous reaches maximum concentration in the mugearites, whereas titanium reaches greatest abundance with the hawaiites. This agrees fairly well with the results of Macdonald (1968), except that he compared these two oxides with

TABLE IV -- Chemical Analyses and Norms (C.I.P.W.) of Average Hawaiian Lavas (After Macdonald, 1968)

SAMPLE NO.	AVNEF	BSITE	BTOID	AVANK	AVAOB	AVHAW	AVMUG	AVTRA
SYMBOL	N	E	D	A	B	H	M	T
SIO2	39.70	44.10	44.80	44.10	45.40	47.90	51.60	61.70
AL203	11.40	12.70	12.70	12.10	14.70	15.90	16.90	18.00
FE203	5.30	3.60	3.20	3.20	4.10	4.90	4.20	3.30
FEO	8.20	9.10	9.40	9.60	9.20	7.60	6.10	1.50
MGO	12.10	11.20	11.40	13.00	7.80	4.80	3.30	0.40
CAO	12.80	10.60	11.40	11.50	10.50	8.00	6.10	1.20
NA2O	3.80	3.60	2.70	1.90	3.00	4.20	5.40	7.40
K2O	1.20	1.00	0.90	0.70	1.00	1.50	2.10	4.20
TIO2	2.80	2.60	2.30	2.70	3.00	3.40	2.40	0.50
P2O5	0.90	0.50	0.50	0.30	0.40	0.70	1.10	0.20
MNO	0.20	0.20	0.20	0.20	0.20	0.20	0.20	0.20
H2O	--	--	--	--	--	--	--	--
CO2	--	--	--	--	--	--	--	--
TOTAL	98.40	99.20	99.50	99.30	99.30	99.10	99.40	98.50
				NORMS (CIPW)				
Q	--	--	--	--	--	--	--	0.2
OR	--	6.0	5.3	4.2	6.0	8.9	12.5	25.2
AB	--	11.1	12.4	11.6	20.5	34.9	45.1	53.5
AN	10.7	15.7	20.0	22.6	23.9	20.3	15.8	3.5
LC	5.7	--	--	--	--	--	--	--
NE	17.7	10.6	5.7	2.5	2.7	0.5	0.5	--
DI								
DIWO	18.0	14.2	14.0	13.7	10.8	6.3	3.1	0.5
DIEN	13.4	9.7	9.3	9.5	6.9	4.2	1.9	0.4
DIFS	2.9	3.4	3.7	3.2	3.2	1.6	1.0	--
HY								
HYEN	--	--	--	--	--	--	--	0.6
HYFS	--	--	--	--	--	--	--	--
OL								
OLFO	12.1	12.9	13.5	16.2	8.8	5.5	4.4	--
OLFA	2.8	5.0	5.8	6.0	4.5	2.4	2.5	--
CS	1.5	--	--	--	--	--	--	--
MT	7.8	5.3	4.7	4.7	6.0	7.2	6.1	4.1
HM	--	--	--	--	--	--	--	0.5
IL	5.4	5.0	4.4	5.2	5.7	6.5	4.6	1.0
AP	2.2	1.2	1.2	0.7	1.0	1.7	2.6	0.5
CC	--	--	--	--	--	--	--	--
TOTAL	100.0	100.0	100.0	100.0	100.0	100.0	100.1	100.0

TABLE V -- Chemical Analyses and Norms (C.I.P.W.) of the Late Stage Volcanic Rocks of Haleakala*

SAMPLE NO.	CA-1	KH-5	AR-6	KH-13	KL-6	PK-1	C-129	C-136
SYMBOL	1	2	3	4	5	6	X	X
SIO2	43.15	43.55	43.40	44.20	43.10	42.55	42.53	42.81
AL203	14.58	14.26	12.48	13.02	14.18	14.42	12.43	14.55
FE203	7.14	3.44	4.65	3.93	3.29	4.30	2.68	4.92
FEO	7.96	10.60	9.28	10.18	11.02	10.16	11.23	10.94
MGO	6.95	8.10	10.70	9.05	7.95	7.75	12.17	5.65
CAO	11.08	11.29	11.84	11.44	11.20	9.78	11.80	9.96
NA20	3.23	3.21	2.47	3.09	2.85	3.04	2.35	3.78
K20	0.90	1.08	0.84	0.96	0.82	1.04	0.81	1.54
TIO2	3.38	3.08	2.88	3.20	3.08	3.44	2.92	3.91
P205	0.42	0.46	0.34	0.43	0.48	0.54	0.55	0.57
MNO	0.22	0.22	0.21	0.21	0.21	0.20	0.16	0.19
H20	0.74	0.41	0.53	0.18	1.31	2.38	0.20	0.71
C02	0.06	0.08	0.30	0.06	0.31	0.08	--	--
TOTAL	99.81	99.78	99.92	99.95	99.80	99.68	99.83	99.54
				NORMS (CIPW)				
Q	--	--	--	--	--	--	--	--
OR	5.3	6.4	5.0	5.7	4.9	6.2	4.8	9.1
AB	18.0	11.2	12.0	13.1	14.7	17.1	5.6	13.9
AN	22.7	21.4	20.5	18.8	23.5	22.7	21.0	18.3
LC	--	--	--	--	--	--	--	--
NE	5.1	8.7	4.8	7.1	5.1	4.7	7.7	9.9
DI								
DIWO	12.2	13.1	14.3	14.5	11.3	9.2	14.2	11.5
DIEN	9.1	7.8	9.8	9.2	6.5	5.7	9.1	6.5
DIFS	1.9	4.6	3.3	4.3	4.2	2.9	4.2	4.6
HY								
HYEN	--	--	--	--	--	--	--	--
HYFS	--	--	--	--	--	--	--	--
OL								
OLFO	5.7	8.7	11.8	9.3	9.3	9.6	14.9	5.4
OLFA	1.3	5.7	4.3	4.8	6.7	5.4	7.5	4.2
CS	--	--	--	--	--	--	--	--
MT	10.4	5.0	6.7	5.7	4.8	6.3	3.9	7.2
HM	--	--	--	--	--	--	--	--
IL	6.4	5.9	5.5	6.1	5.9	6.6	5.5	7.5
AP	1.0	1.1	0.8	1.0	1.1	1.3	1.3	1.4
CC	0.1	0.2	0.7	0.1	0.7	0.2	--	--
TOTAL	99.3	99.6	99.5	99.8	98.7	97.6	99.8	99.3

*See Table III for sources of data.

TABLE V (Continued) Chemical Analyses and Norms (C.I.P.W.) of the Late Stage Volcanic Rocks of Haleakala*

SAMPLE NO.	C-138	C-139	C-142	C-148	C-146	C-147	C-156	46PB1
SYMBCL	X	X	X	X	O	O	O	O
SIO2	42.46	41.55	41.46	42.86	46.00	44.54	44.46	42.30
AL203	12.57	14.13	14.11	16.20	14.48	16.51	13.97	10.52
FE203	4.90	3.99	6.05	7.55	4.50	2.88	6.14	4.22
FEO	9.98	11.36	10.22	6.62	8.85	10.58	8.95	9.70
MGO	9.37	6.04	6.74	7.24	4.90	5.64	5.41	14.90
CAO	11.77	11.79	10.56	10.77	8.44	8.31	10.28	12.08
NA2O	2.96	3.84	3.36	3.19	4.89	4.46	3.07	1.56
K2O	1.27	1.67	1.33	1.55	1.84	1.57	1.17	0.42
TIO2	3.08	4.10	4.24	1.84	3.63	3.68	4.08	2.41
P2O5	0.45	0.63	0.52	0.56	0.72	0.62	0.72	0.33
MNO	0.17	0.19	0.21	0.19	0.21	0.20	0.20	0.06
H2O	0.44	0.28	0.88	0.97	1.15	0.58	1.35	1.32
CO2	--	--	--	--	--	--	--	--
TOTAL	99.42	99.57	99.68	99.54	99.61	99.57	99.80	99.82
				NORMS (CIPW)				
Q	--	--	--	--	--	--	--	--
OR	7.5	9.9	7.9	9.2	10.9	9.3	6.9	2.5
AB	6.3	2.8	11.4	12.6	23.9	19.4	25.4	7.1
AN	17.4	16.5	19.6	25.4	12.2	20.5	20.9	20.5
LC	--	--	--	--	--	--	--	--
NE	10.2	16.1	9.3	7.9	9.6	10.0	0.4	3.3
DI								
DIWO	16.0	15.9	12.4	10.3	10.5	7.0	10.6	15.6
DIEN	10.6	8.8	8.1	7.8	6.3	3.8	7.2	11.1
DIFS	4.3	6.5	3.4	1.4	3.6	3.0	2.7	3.1
HY								
HYEN	--	--	--	--	--	--	--	--
HYFS	--	--	--	--	--	--	--	--
OL								
OLFO	9.0	4.4	6.2	7.2	4.1	7.2	4.4	18.3
OLFA	4.1	3.6	2.9	1.4	2.6	6.4	1.8	5.7
CS	--	--	--	--	--	--	--	--
MT	7.1	5.8	8.8	11.0	6.6	4.2	8.9	6.1
HM	--	--	--	--	--	--	--	--
IL	5.9	7.8	8.1	3.5	6.9	7.0	7.8	4.6
AP	1.1	1.5	1.2	1.3	1.7	1.5	1.7	0.8
CC	--	--	--	--	--	--	--	--
TOTAL	99.6	99.8	99.1	99.1	98.9	99.5	98.7	98.7

*See Table III for sources of data.

TABLE V (Continued) Chemical Analyses and Norms (C.I.P.W.) of the Late Stage Volcanic Rocks of Haleakala*

SAMPLE NO.	C-127	C-135	C-137	C-140	C-141	C-143	C-144	C-145
SYMBOL	O	O	O	O	O	O	O	O
SIO2	47.26	40.51	46.31	44.72	51.90	45.66	47.48	44.76
AL2O3	17.19	13.80	15.29	13.86	17.10	17.01	16.32	15.22
FE2O3	2.87	5.73	4.02	5.69	3.38	4.96	6.18	3.96
FEO	9.35	10.30	8.84	9.82	6.64	7.73	6.32	10.34
MGO	5.08	6.32	4.86	5.07	2.26	4.60	3.96	5.74
CAO	7.82	12.02	9.76	10.89	5.70	8.09	7.34	8.40
NA2O	3.50	3.53	3.72	3.07	6.65	5.01	4.00	3.71
K2O	1.40	1.50	1.47	1.09	2.72	1.55	1.41	1.13
TIO2	3.58	4.15	3.67	3.96	2.11	3.41	3.50	4.63
P2O5	0.77	0.56	0.74	0.61	0.84	0.75	0.71	0.56
MNO	0.22	0.19	0.19	0.23	0.17	0.20	0.21	0.20
H2O	0.86	0.89	0.77	0.73	0.63	0.77	1.58	0.98
CO2	--	--	--	--	--	--	--	--
TOTAL	99.91	99.50	99.64	99.74	100.10	99.74	99.81	99.63
				NORMS (CIPW)				
Q	--	--	--	--	--	--	0.3	--
OR	8.3	8.9	8.7	6.5	16.1	9.2	8.3	6.7
AB	29.6	3.2	26.0	23.4	37.4	26.2	33.9	27.2
AN	27.1	17.5	20.8	20.9	8.8	19.4	22.5	21.6
LC	--	--	--	--	--	--	--	--
NE	--	14.5	3.0	1.4	10.2	8.8	--	2.4
DI								
DIWO	2.8	16.2	9.6	12.2	5.8	6.7	3.9	6.9
DIEN	1.6	10.2	5.7	7.4	2.7	4.4	2.9	4.1
DIFS	1.1	5.0	3.4	4.2	3.0	1.8	0.6	2.4
HY								
HYEN	3.8	--	--	--	--	--	7.0	--
HYFS	2.8	--	--	--	--	--	1.4	--
OL								
OLFO	5.1	3.9	4.5	3.7	2.0	5.0	--	7.2
OLFA	4.2	2.1	3.0	2.3	2.5	2.3	--	4.7
CS	--	--	--	--	--	--	--	--
MT	4.2	8.3	5.8	8.3	4.9	7.2	9.0	5.8
HM	--	--	--	--	--	--	--	--
IL	6.8	7.9	7.0	7.5	4.0	6.5	6.7	8.8
AP	1.8	1.3	1.8	1.4	2.0	1.8	1.7	1.3
CC	--	--	--	--	--	--	--	--
TOTAL	99.2	99.1	99.3	99.3	99.4	99.3	98.2	99.0

*See Table III for sources of data.

TABLE V (Continued) Chemical Analyses and Norms (C.I.P.W.) of the Late Stage Volcanic Rocks of Haleakala*

SAMPLE NO.	46A2	46A3	46A4	46A5	460A6	AUG	C137G	C141G
SYMBOL	O	O	O	O	O	+	+	+
SIO2	46.90	46.94	47.64	47.78	54.14	47.70	48.70	50.60
AL203	16.60	16.54	17.62	16.32	17.82	6.82	5.60	4.20
FE203	4.37	5.31	5.62	4.37	3.90	3.36	--	--
FEO	7.16	7.16	5.48	8.43	5.34	4.43	8.20	8.80
MGO	4.35	4.33	4.19	5.06	1.88	13.34	13.00	12.80
CAO	8.50	8.34	7.90	7.58	4.94	21.35	21.60	22.20
NA20	4.51	4.27	4.72	4.18	6.24	0.65	0.47	0.54
K20	2.38	1.49	1.60	1.30	2.72	0.03	--	--
TIO2	3.92	4.05	3.44	4.11	1.81	1.89	2.40	1.90
P205	0.79	0.71	0.87	0.61	0.61	--	--	--
MNO	0.07	0.07	0.08	0.08	0.08	0.16	0.17	0.33
H20	0.24	0.51	0.54	0.43	0.27	0.15	--	--
C02	--	--	--	--	--	--	--	--
TOTAL	99.79	99.72	99.70	100.25	99.75	99.88	100.14	101.37
				NORMS (CIPW)				
Q	--	--	--	--	--	--	--	--
OR	14.1	8.8	9.5	7.7	16.1	--	--	--
AB	24.4	32.8	35.0	35.3	46.8	--	--	0.5
AN	18.1	21.6	22.2	21.9	12.6	15.6	13.2	8.9
LC	--	--	--	--	--	0.1	--	--
NE	7.5	1.8	2.7	--	3.3	3.0	2.2	2.1
DI								
DIWO	7.9	6.4	4.8	4.9	3.3	37.5	38.0	41.6
DIEN	5.6	4.8	4.1	3.2	1.8	30.6	25.9	27.2
DIFS	1.7	1.0	--	1.3	1.4	2.3	9.1	11.6
HY								
HYEN	--	--	--	0.7	--	--	--	--
HYFS	--	--	--	0.3	--	--	--	--
OL								
OLFO	3.7	4.2	4.5	6.1	2.0	1.9	4.5	3.0
OLFA	1.2	1.0	--	2.8	1.8	0.2	1.8	1.4
CS	--	--	--	--	--	0.2	0.9	--
MT	6.3	7.7	8.0	6.3	5.7	4.9	--	--
HM	--	--	0.1	--	--	--	--	--
IL	7.5	7.7	6.6	7.8	3.4	3.6	4.6	3.6
AP	1.9	1.7	2.1	1.4	1.4	--	--	--
CC	--	--	--	--	--	--	--	--
TOTAL	99.8	99.5	99.5	99.6	99.8	99.9	100.0	100.0

*See Table III for sources of data.

TABLE V (Continued) Chemical Analyses and Norms (C.I.P.W.) of the Late Stage Volcanic Rocks of Haleakala*

SAMPLE NO.	C139G	C142G	C148G
SYMBOL	+	+	+
SIO2	45.00	46.00	46.50
AL203	8.50	7.10	6.80
FE203	--	--	--
FEO	8.20	8.30	7.90
MGO	11.20	11.70	12.80
CAO	22.90	22.30	22.40
NA2O	0.43	0.49	0.42
K2C	--	--	--
TIO2	3.80	3.40	2.70
P2O5	--	--	--
MNO	0.14	0.13	0.12
H2O	--	--	--
CO2	--	--	--
TOTAL	100.17	99.42	99.64
	NORMS (CIPW)		
Q	--	--	--
OR	--	--	--
AB	--	--	--
AN	21.2	17.3	16.7
LC	--	--	--
NE	2.0	2.3	1.9
DI			
DIWO	28.2	32.2	31.8
DIEN	19.5	22.1	22.1
DIFS	6.3	7.5	7.1
HY			
HYEN	--	--	--
HYFS	--	--	--
OL			
OLFO	5.8	5.0	6.9
OLFA	2.1	1.9	2.5
CS	7.6	5.2	5.7
MT	--	--	--
HM	--	--	--
IL	7.2	6.5	5.1
AP	--	--	--
CC	--	--	--
TOTAL	100.0	100.0	100.0

*See Table III for sources of data.

sodium and not magnesium as done here. The rocks of the Kula Formation show consistently increasing calcium and total iron and decreasing potassium, sodium, silica and aluminum with increasing magnesium. Hana lavas are generally richer in magnesium than Kula rock. Calcium only increases slightly with increasing magnesium. Other oxides either decrease slightly or remain nearly constant with increasing magnesium content.

In general, the lavas of the Kula Formation follow a trend very similar to that of the oceanic basalt-trachyte association, which appears to be controlled largely by crystal differentiation (Macdonald and Katsura, 1964). The Kula Formation, however, consists predominantly of hawaiites and basalts, with only a very few mugearites. Only a single dike of trachyte has been found on Haleakala (Macdonald, verbal communication, 1977). If, in fact, the Kula lavas do follow the alkalic trend, it appears that volcanic activity or igneous differentiation ceased partially through the series.

Hana lavas chemically show many slight differences from the Kula lavas. Some of the more important differences are that Hana rocks, as compared to Kula lavas, are relatively enriched in calcium, iron, and especially magnesium. Possibly even more distinctive is the silica deficiency of the Hana lavas, which contain between 4.7 to 16.1 percent normative nepheline. The lavas of the Hana

Formation, however, are less understaurated in silica than the post-erosional nephelinites of other Hawaiian volcanoes (Figure 4).

It has been suggested that the same processes that formed the post-erosional lavas of other Hawaiian volcanoes also produced the lavas of the Hana Formation, but that these processes have operated over a much shorter period of time (Macdonald and Powers, 1968). The overlap of chemical trends between the Kula lavas and the post-erosional Hana lavas, along with the excellence of outcrop quality and lack of any major unconformities in the map area indicate that along the southwest rift zone, the time interval between the two formations was quite short.

Various writers have indicated that depth of formation or depth at which fractionation takes place may be the predominant factors in determining the compositions of magmas.

Green (1969) indicates that at low pressures (depths of less than 10-15 km) fractionation is common and could be a factor in divergence of the alkalic basalt-trachyte association from the tholeiitic suite. Fractionation of mantle material at depths of between 40-70 km would produce magma of olivine basanite or olivine nephelinite compositions, whereas magma from 60-100 km depths might produce olivine nephelinites or olivine melilite nephelinites (Green, 1969).

Macdonald (1968) points out that the three major rock suites (tholeiitic, alkalic, and nephelinic) are chemically intergradational. Crystallization of a magma of olivine tholeiite composition at shallow depth would produce a tholeiitic magma. At somewhat greater depths, due to late stage consolidation of the upper portions of the magma chamber, the higher pressures would produce alkalic magmas. At depths of several tens of kilometers nephelinic magmas would be produced (Macdonald, 1968).

Studies by Kushiro (1965, 1969), Yoder and Tilley (1961, 1962), and others also suggest that high pressures are needed to produce a silica-poor, alkali-rich magma. Experiments on the effects of various ions on the shift of liquidus boundaries indicate that in fractional crystallization of olivine and pyroxene, enrichment in silica would occur in the magma in the presence of moderately large amounts of oxides of monovalent cations (H_2O, Na_2O, and K_2O) at low pressures. In the presence of oxides of polyvalent cations (CO_2, TiO_2 and P_2O_5) the magma would be poorer in silica. At high pressures, the magma would become less silicic, even in the presence of monovalent cations (Kushiro, 1975).

Figure 4 is a plot of SiO_2 against $TiO_2 + P_2O_5$ for the late stage lavas of Haleakala. Trends of the Kula Formation and the Hana Formation are shown by least squares lines. In calculating the Kula trend, sample 46PB1 was not used. As a probable cumulate (picrite

basalt), it lies far from the rest of the data. Correlation coefficients were calculated giving r = 0.57 for the Hana lavas and r = 0.62 for the Kula lavas. For both formations, as the polyvalent cation concentration increases, the silica content decreases, as expected.

Figure 5 is the alkali:silica diagram for these same lavas. Sample C-135, a basanitoid lying well off the Kula trend, was not used to calculate the regression line for the Kula lavas. Correlation coefficients are r = 0.48 for the Hana Formation and r = 0.86 for the Kula Formation. As can be seen in Figure 5, as alkalis (monovalent cations) increase so does silica for the Kula lavas. For the Hana lavas, although not a very good fit, the amount of monovalent cations, Na_2O and K_2O, increases as silica content decreases.

This indicates then, that the lavas of the Kula Formation were differentiated at, and erupted from, a relatively shallow depth. The later Hana Formation lavas were probably produced at a depth and pressure sufficiently great to keep the magma silica-poor in the presence of appreciable amounts of alkalis. Although this fact and the high normative nepheline content suggest that Hana lavas are nephelinic, it should be noted that nepheline was not found in the mode of any samples studied. Macdonald (1968) has said that the silica deficiency is probably in the pyroxene.

Figure 4. Plot of SiO_2 against $TiO_2 + P_2O_5$, late stage volcanic rocks of Haleakala. Least squares fit of data shown by light dashed lines. Hana: r = 0.57. Kula: r = 0.62; sample 46PB1 was deleted. Plotting symbols as shown in Table III.

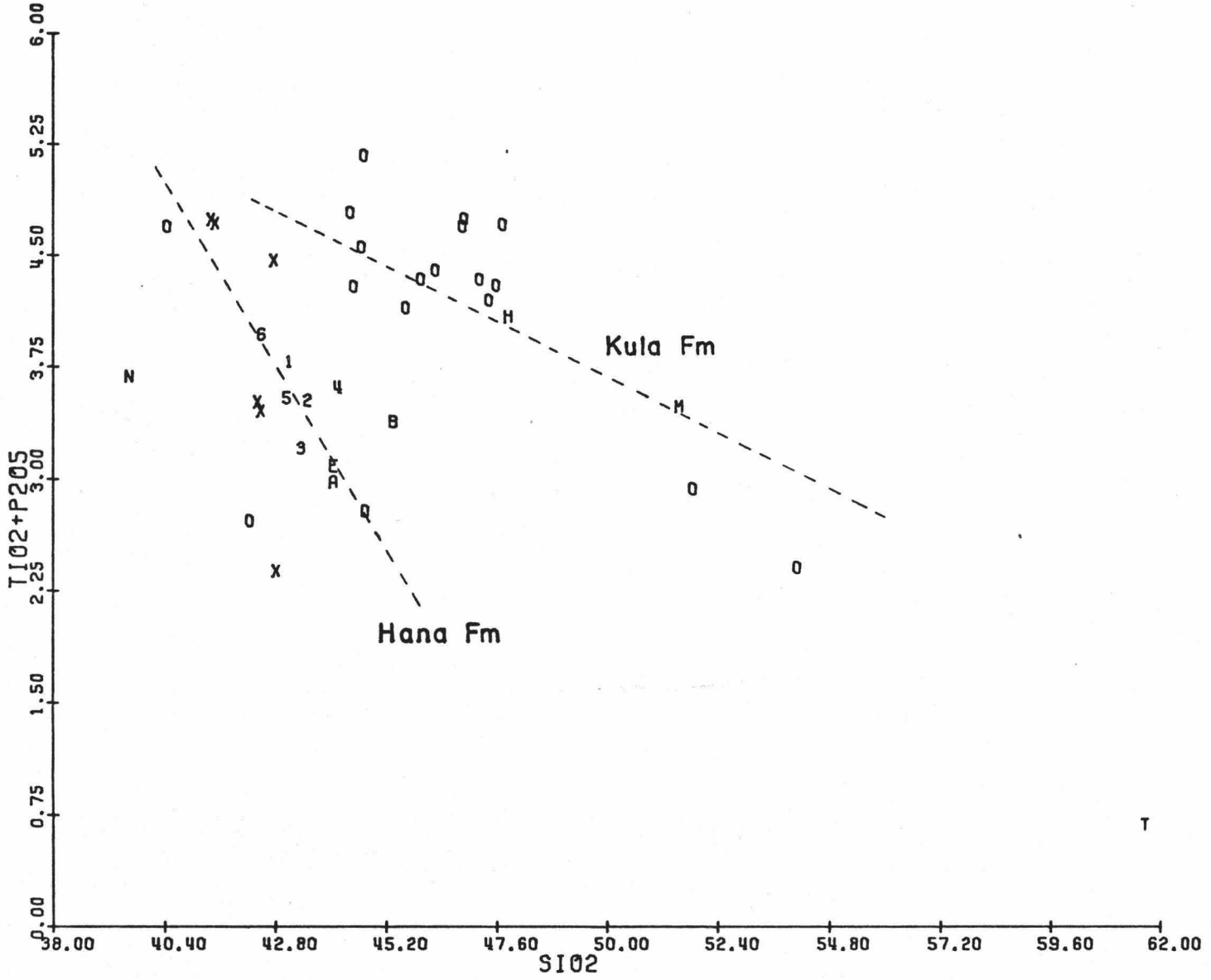
TI02+P205
SI02
0.00
0.75
1.50
2.25
3.00
3.75
4.50
5.25
6.00
38.00
40.40
42.80
45.20
47.60
50.00
52.40
54.80
57.20
59.60
62.00
Kula Fm
Hana Fm

Figure 5. Alkali:silica diagram of the late stage lavas of Haleakala, showing the boundary (heavy dashed line) between the tholeiitic and alkalic fields (Macdonald, 1968). Least squares fit of data shown by light dashed lines. Hana: $r = 0.48$. Kula: $r = 0.86$; sample C-135 was deleted. Plotting symbols as shown in Table III.

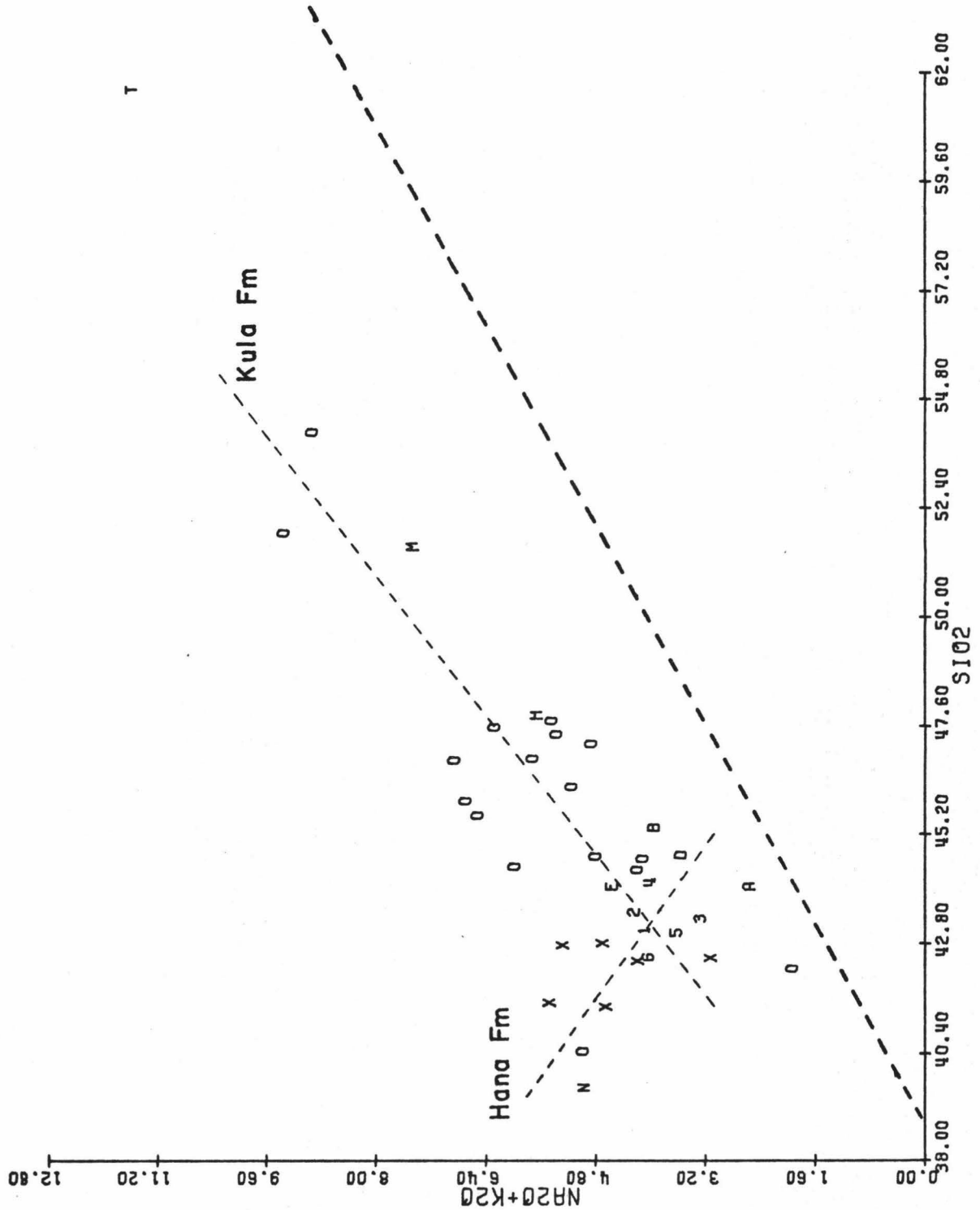
Kula Fm
Hana Fm
SIO2
NA2O+K2O
38.00
40.40
42.80
45.20
47.60
50.00
52.40
54.80
57.20
59.60
62.00
0.00
1.60
3.20
4.80
6.40
8.00
9.60
11.20
12.80

Similar to the relation of the Kula lavas and the alkalic trend, the Hana lavas began along the nephelinic trend but eruptions ceased before the magma reached a truly nephelinic composition.

Figure 6 is an AFM diagram on which, in addition to the late stage lavas of Haleakala, average Hawaiian alkalic rocks, and six Haleakala pyroxene phenocrysts (Tables III, IV, and V), is plotted an olivine of calculated Fo_{85} composition, based on the estimated average olivine composition in thin section. The late stage lavas of Haleakala follow the variation trend of the average Hawaiian rocks, but within a limited range. The variation of lavas of the Hana Formation appears to be controlled by movement of olivine or pyroxene crystals within the magma (Macdonald and Powers, 1968). The trend of the Kula lavas may be controlled by olivine and pyroxene to a lesser extent, whereas fractionation of feldspar may play a correspondingly more important role (see Figure 7).

Figure 6. Ternary plot of $Na_2O + K_2O$, FeOT, and MgO (AFM diagram), late stage volcanic rocks of Haleakala. Plotting symbols as shown in Table III. FeOT = FeO + 0.89981 x Fe_2O_3 + MnO. L is olivine of calculated Fo_{85} composition. The dashed line indicates the variation trend of average Hawaiian rocks.

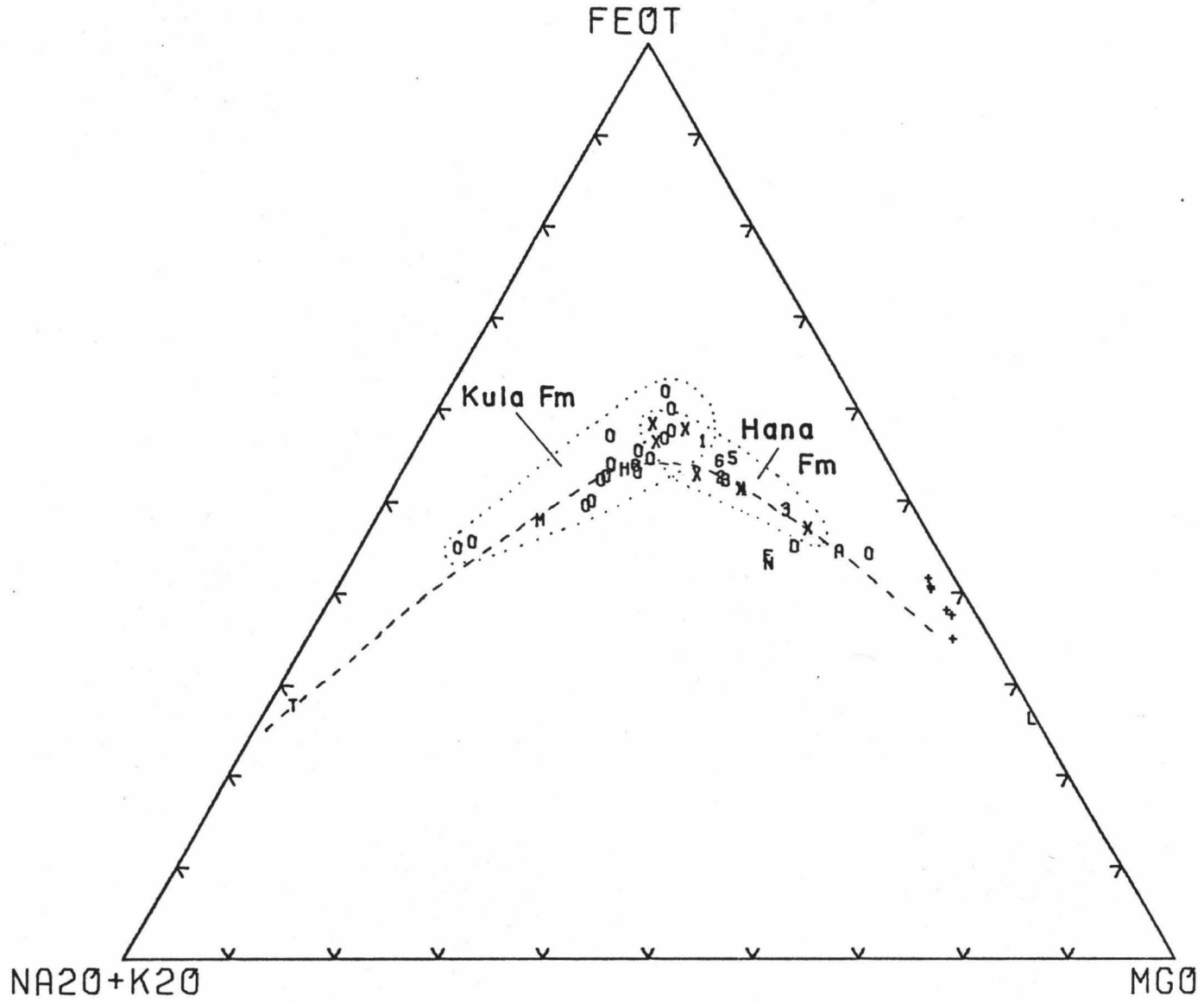
FE0T
Kula Fm
Hana
Fm
NA20+K20
MG0

Figure 7. Ternary plot of Na_2O, K_2O, and CaO, late stage lavas of Haleakala. Plotting symbols as shown in Table III.

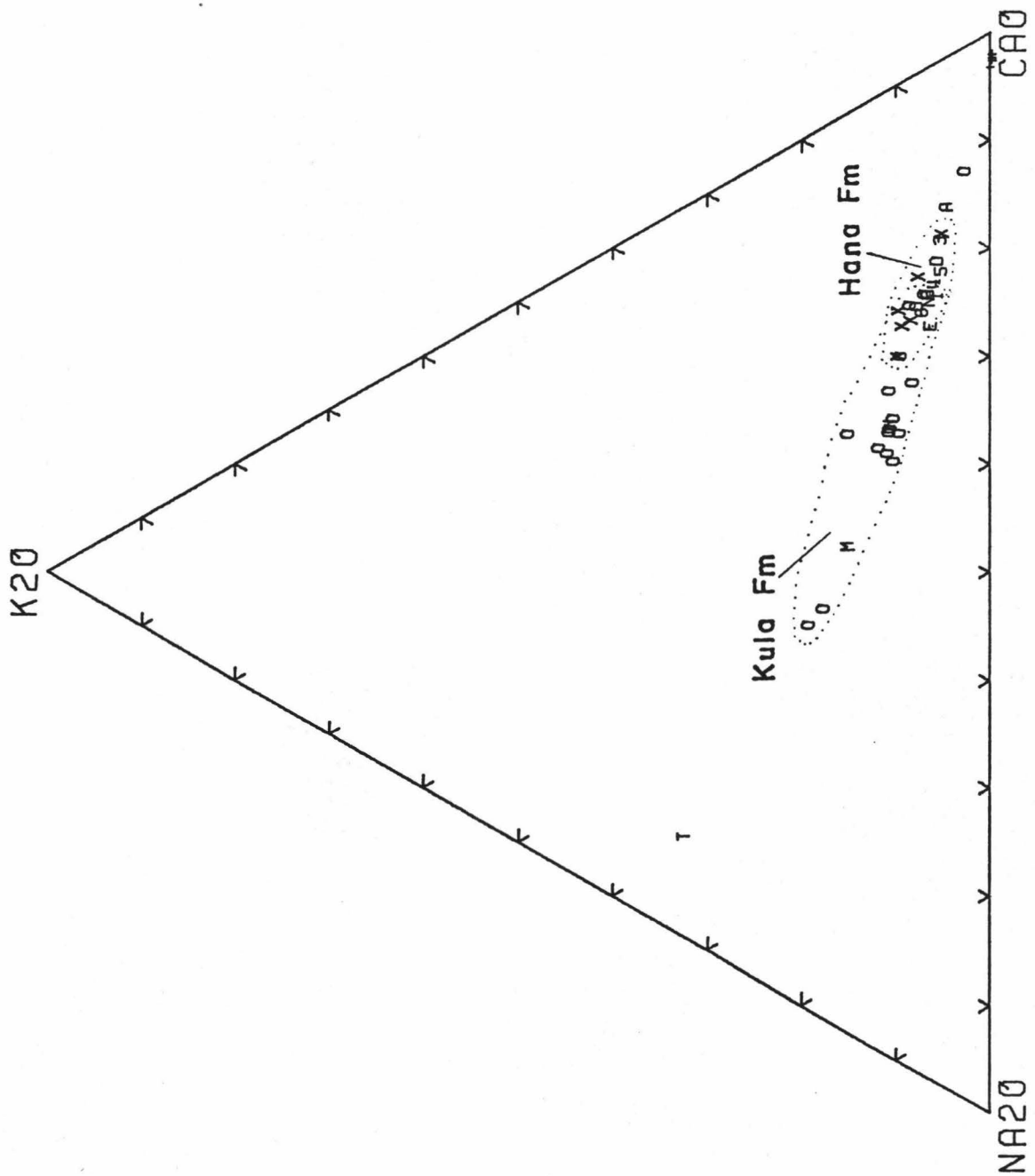
K2O
CAO
NA2O
Hana Fm
Kula Fm

SUMMARY AND CONCLUSIONS

The upper southwest rift zone of Haleakala consists of two formations of late stage volcanic rocks. There is no strong evidence to indicate that an appreciable interval of quiescence occurred between the two formations, as apparently did happen on other parts of the volcano. Volcanic activity on the southwest rift zone appears to have been nearly continuous from the time of eruption of Kula lavas until recent times. McDougall (1964) indicates that for Haleakala as a whole, Kula activity commenced about 0.84 m.y. ago, whereas Hana lavas are at least younger than 0.45 m.y.

In terms of rock types present, both the Kula and the Hana lavas exposed on the southwest rift tend to follow the trends and compositions as suggested by earlier writers (Stearns and Macdonald, 1942; Macdonald and Powers, 1946, 1968). However, the hawaiites are more mafic and less silicic than most hawaiites from other parts of Haleakala. Hana lavas are predominantly alkalic olivine basalts sufficiently poor in silica for most to be classified as basanitoids. Many are enriched in mafic components, especially in large phenocrysts of augite and olivine, and grade into picritic basalts of the ankaramite type. Both formations, for the most part, belong to the alkalic suite, although the Hana Formation is possibly transitional to the nephelinic suite.

The Hana lavas and extensive cover of pyroclastic debris have buried all but a few isolated exposures of Kula rocks south of the rift zone. Those lavas that are exposed are probably among the last lavas of the Kula Formation to be erupted. Dating of these lavas might prove of use in determining the time interval between the two formations, with possible application to theories of petrogenesis.

APPENDIX A. -- Descriptions of Sample Locations*

Sample	Locality
AR-2	Alkalic olivine basalt; aa, 15 m upslope from access road through Kula Forest Reserve; 1.0 km northeast of junction of road to Polipoli Springs and access road; overlain by thin layer of cinder and ash; Hana Formation.
AR-3	Ankaramite; aa, from collapsed lava tube 1.6 km northeast of junction of road to Polipoli Springs and access road, at edge of road; Hana Formation.
AR-6	Ankaramite; large block of aa, 150 m northeast of trail to spatter cone located 0.5 km southeast of access road; Hana Formation.
AR-8	Picrite basalt, transitional to ankaramite; 1.9 km northeast of junction of access road and Polipoli Springs Road, in roadcut; from clinkery portion of aa; Hana Formation.
AR-9	Alkalic olivine basalt, transitional to ankaramite; 2.1 km northeast of junction of Polipoli Springs and access road; aa exposed by road; Hana Formation.
AR-11	Alkalic olivine basalt; 2.5 km from junction of road to Polipoli Springs and access road; aa flow overlain by 9 m of Kula ash and soil and Hana ash in roadcut; Kula Formation.
AR-12	Alkalic olivine basalt; dense portion of aa flow interbedded with weathered Kula ash, 0.3 km north of sample AR-11, in roadcut; Kula Formation.
AR-13	Ankaramite; aa, 2 m from southern base of spatter cone, 0.5 km southeast of access road on trail; Hana Formation.
P-2	Alkalic olivine basalt; poorly exposed weathered aa flow at head of small gorge 130 m southeast of benchmark at Polipoli; Kula Formation.
P-4	Alkalic olivine basalt; 6-9 m thick section of dense aa flow exposed inside "Cave Shelter" on southern slope of Polipoli; Kula Formation.
HP-3	Alkalic olivine basalt; highly vesicular pahoehoe mantling small spatter cone at vent, 0.7 km east of benchmark at Polipoli; Hana Formation.

* See Figure 2 for locations.

APPENDIX A (Continued) Descriptions
Of Sample Locations

Sample	Locality
HP-4	Scoria (alkalic olivine basalt); moderately dense scoria, in deep roadcut from cinder cone, 0.3 km southeast of Polipoli Springs; Hana Formation.
T-1	Ankaramite, transitional to alkalic olivine basalt; dense aa from tumulus 1.0 km east of Polipoli; Hana Formation.
T-2	Ankaramite, transitional to alkalic olivine basalt; aa transitional from pahoehoe; same flow as sample T-1; sample from tumulus-like feature 1.2 km east of Polipoli at base of steep slope of Kula cinder; Hana Formation.
PK-1	Cinder; fresh, from roadcut about 330 m south of the summit of Puu Keokea; Hana Formation.
PK-3	Alkalic olivine basalt; very small exposure of extremely vesicular pahoehoe in depression just east of Puu Keokea; Hana Formation.
BP-3	Alkalic olivine basalt, transitional to ankaramite; 200 m southeast of remnant of spatter cone near junction of road to Kahua and road up rift to summit; sample is aa, but locally flow is pahoehoe; Hana Formation.
BP-4	Alkalic olivine basalt, transitional to ankaramite; aa, 100 m west of sample BP-3; Hana Formation.
BP-9	Hawaiite, transitional to alkalic olivine basalt; small exposure of very dense, blocky aa 300 m southeast of Puu Keokea; Kula Formation.
DC-9	Ankaramite; pahoehoe flow on northern slope of large cone 1.4 km east of Puu Keokea; sample obtained 0.4 km northwest of summit of large cone; Hana Formation.
KH-2	Alkalic olivine basalt, transitional to alkalic basalt; weathered pahoehoe from eastern side of Kahua cinder cone; Hana Formation.
KH-4	Alkalic olivine basalt; 150 m northeast of hunter's shelter just north of Kahua; dense aa flow; Hana Formation.

APPENDIX A (Continued) Descriptions
Of Sample Locations

Sample	Locality
KH-5	Picrite basalt; clinkery aa about 10 m northeast of shelter at Kahua; Kula Formation.
KH-10	Alkalic olivine basalt; outer portion of accretionary lava ball; core is from nearby Kula spatter-cinder cone; 200 m north of road to Kahua; Hana Formation.
KH-13	Alkalic olivine basalt; 1 m thick aa flow, sample from roadcut 1.4 km west of hunter's shelter at Kahua; Hana Formation.
KH-14	Ankaramite; 0.8 km west of sample KH-13 location, in roadcut; predominately pahoehoe, locally aa; Hana Formation.
KH-15	Alkalic olivine basalt, transitional to picrite basalt; 2.0 km east of junction of road to Kahua and ridge road, clinkery pahoehoe at edge of road; Hana Formation.
KH-16	Alkalic olivine basalt, transitional to picrite basalt; aa immediately upslope of road to Kahua, 1.5 km east of junction of road and ridge road; Hana Formation.
KH-17	Alkalic olivine basalt; aa, 1.2 km east of junction in cut on road to Kahua; Hana Formation.
KH-19	Alkalic olivine basalt; aa, 0.9 km east of Kahua shelter at edge of trail; Hana Formation.
KH-21	Hawaiite, transitional to alkalic olivine basalt; dense aa, about 1.3 m thick, 1.0 km N 30° W from hunter's shelter at Kahua and 200 m east of fresh black lava flow from near Kalepeamoa; Kula Formation.
KH-22	Alkalic olivine basalt, transitional to alkalic basalt; from stream bed 0.3 km west of hunter's shelter; Hana Formation.
PA-2	Ankaramite; pahoehoe, 15 m north of small spatter rampart on surface of flow northwest of Kanahau cinder cone; Hana Formation.

APPENDIX A (Continued) Descriptions
Of Sample Locations

Sample	Locality
KN-4	Ankaramite; from lava channel 400 m southeast of benchmark at Kanahau; Hana Formation.
KN-5	Ankaramite; pahoehoe 0.5 km south of benchmark at Kanahau; Hana Formation.
KL-1	Alkalic olivine basalt, transitional to hawaiite; aa, at Kalepeamoa, 10 m north of ridge road; Kula Formation.
KL-4	Alkalic olivine basalt, transitional to hawaiite; dense aa, from kipuka about 50 m east of large fresh cinder cone south of Kalepeamoa; Kula Formation.
KL-6	Alkalic olivine basalt, transitional to alkalic basalt; sample from vent of cinder cone located 0.4 km south of Kalepeamoa; Hana Formation.
KL-7	Alkalic olivine basalt; aa, 0.3 km west of Kalepeamoa, near large gully; Kula Formation.
KL-11	Glass block; on surface of cinder and block strewn field, 1.0 km northeast of Kalepeamoa, about 20 m from edge of exposed flow.
CA-1	Hawaiite, transitional to alkalic olivine basalt; dense, blocky aa from crescentic exposure at southern edge of small cinder cone where CAA Repeater Station is located; Kula Formation.
CA-6	Hawaiite, transitional to alkalic olivine basalt; aa, exposed at edge of large pit crater about 150 m north of small twin cinder cones and 0.9 km southwest of CAA Repeater Station; Kula Formation.
CA-8	Ankaramite, transitional to alkalic olivine basalt; pahoehoe from eastern side of lava channel near vent of twin cinder cones, 1.0 km southwest of the CAA Repeater Station; Hana Formation.
CA-12	Alkalic olivine basalt, transitional to alkalic basalt; blockly flow 75 m northwest of road and 1.1 km northeast of Kalepeamoa; Kula Formation.
CA-13	Alkalic olivine basalt; dense portion of thick aa flow overlain by welded red cinder and spatter, on ridge crest 0.8 km east of Kalepeamoa; Kula Formation.

APPENDIX B. Magnesia chemical variation diagrams (Figures 8-15) for the late stage lavas of Haleakala, Maui. Included are average Hawaiian lavas and six pyroxene phenocrysts. Plotting symbols are given in Table III.

Figure 8. Plot of MgO against K_2O.

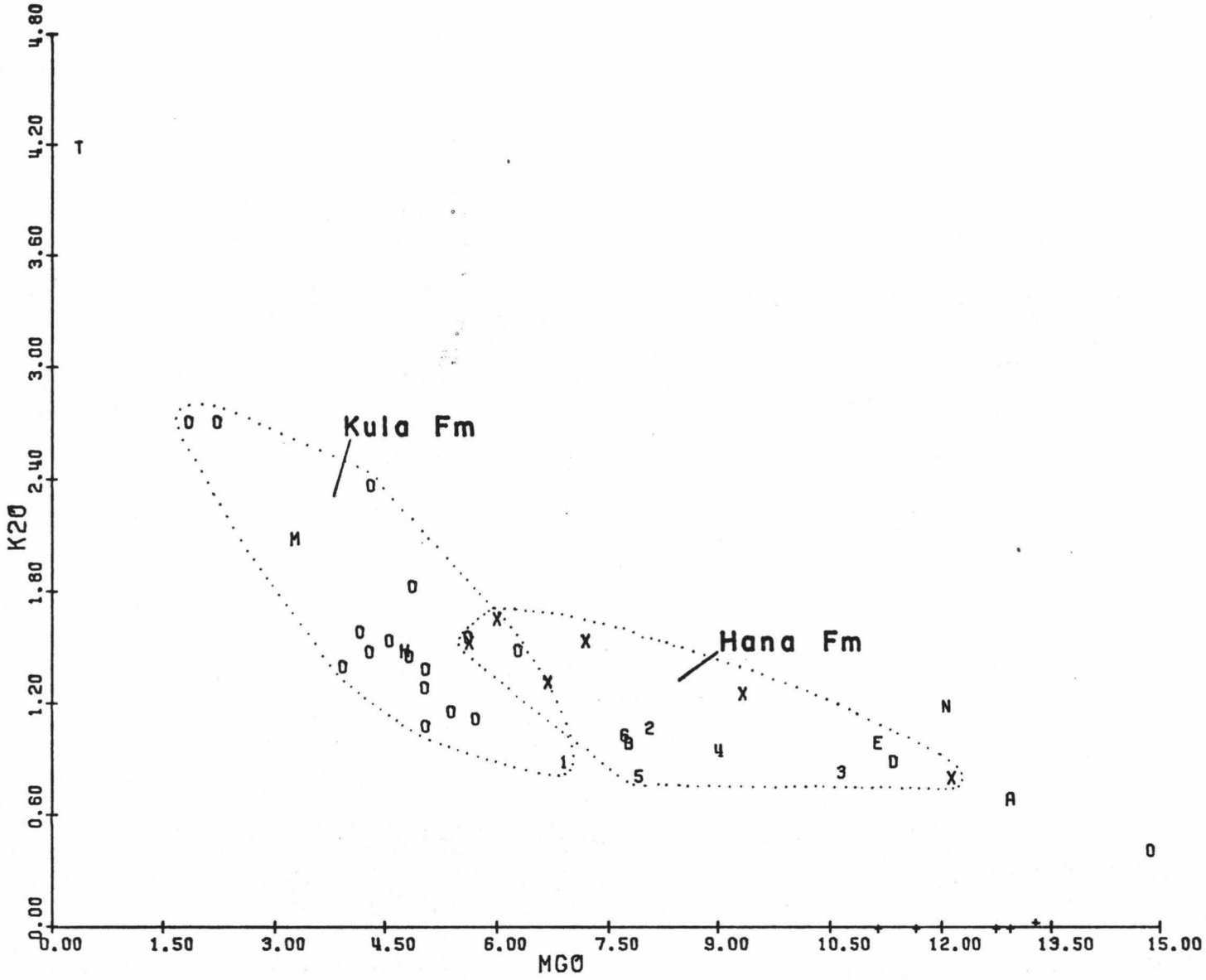
Kula Fm
Hana Fm
K2O
MGO
0.00
0.60
1.20
1.80
2.40
3.00
3.60
4.20
4.80
0.00
1.50
3.00
4.50
6.00
7.50
9.00
10.50
12.00
13.50
15.00

Figure 9. Plot of MgO against Na_2O.

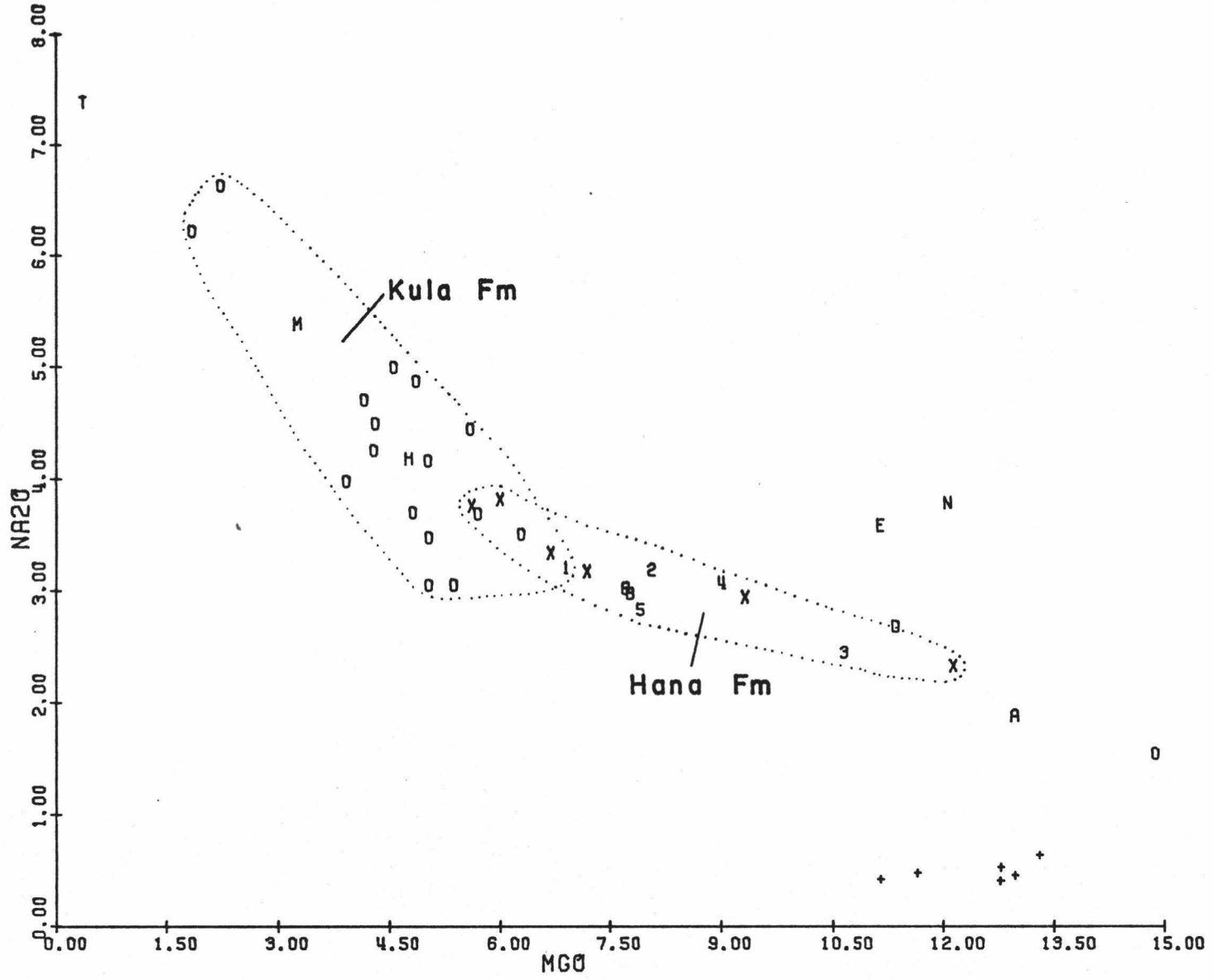
Kula Fm
Hana Fm
NA2O
MGO
0.00
1.00
2.00
3.00
4.00
5.00
6.00
7.00
8.00
0.00
1.50
3.00
4.50
6.00
7.50
9.00
10.50
12.00
13.50
15.00

Figure 10. Plot of MgO against CaO.

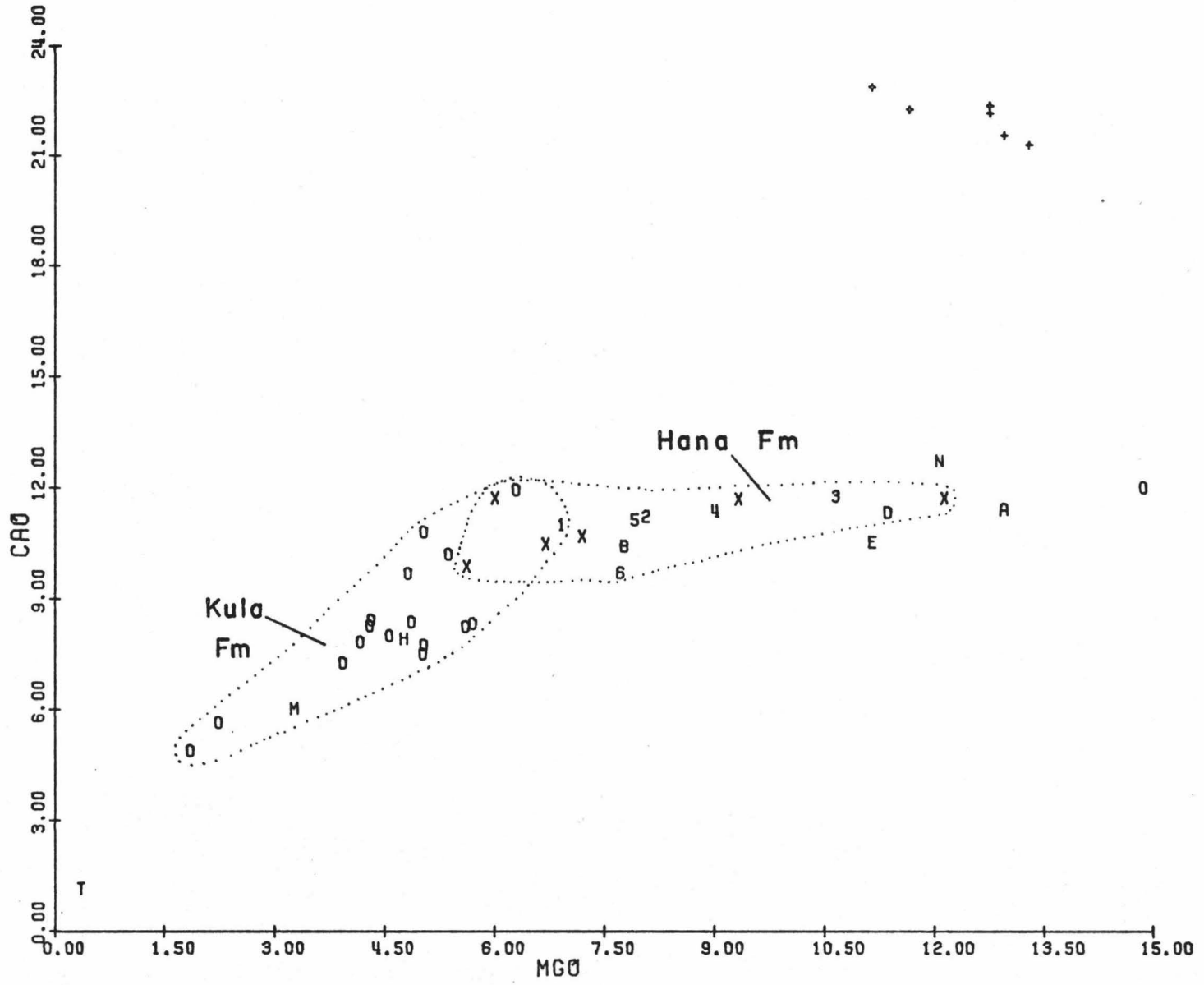
Hana Fm
Kula
Fm
CAO
MGO
0.00
3.00
6.00
9.00
12.00
15.00
18.00
21.00
24.00
1.50
4.50
7.50
10.50
13.50

Figure 11. Plot of MgO against FeOT. FeOT = FeO + 0.89981 x Fe_2O_3 + MnO.

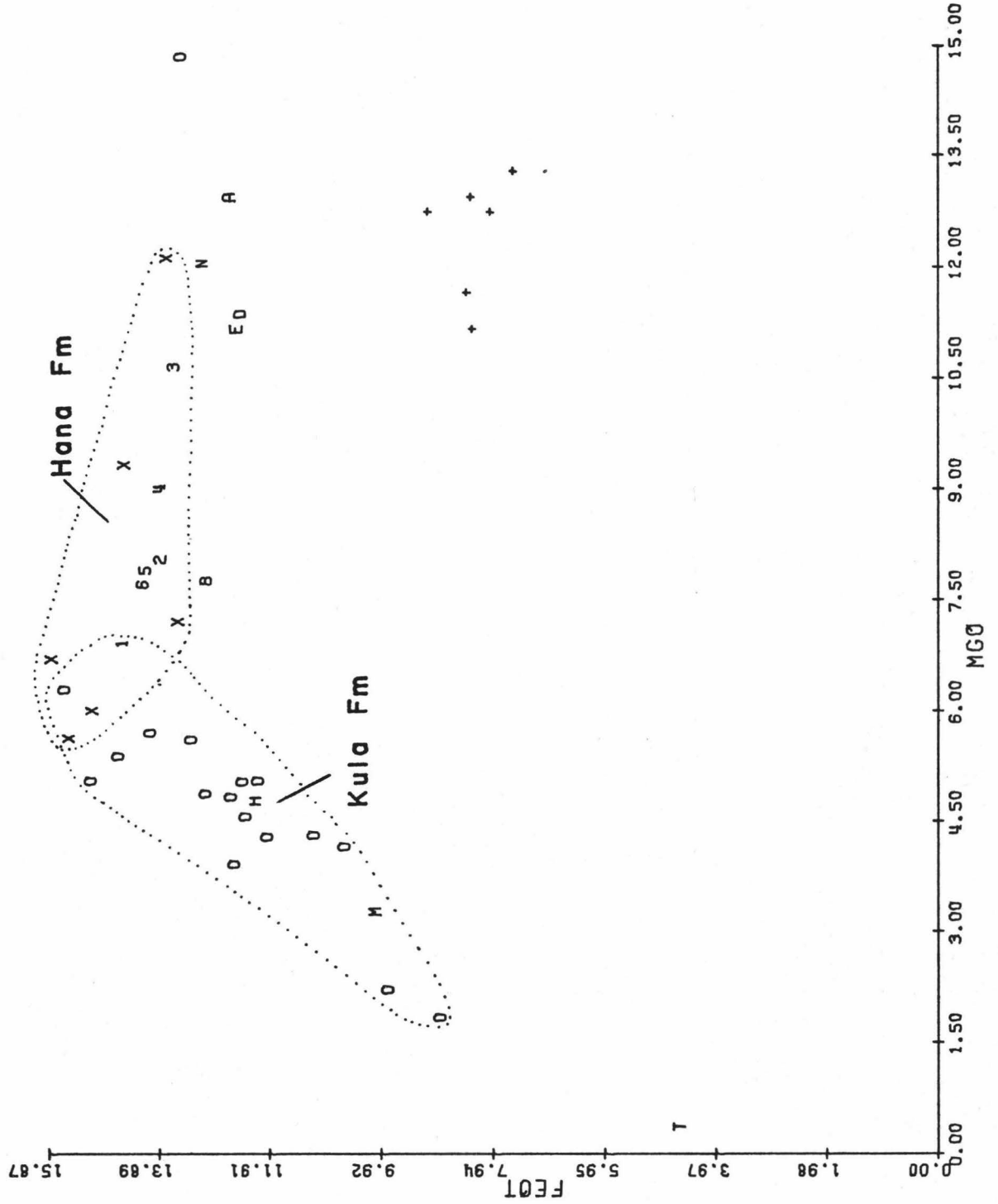
Hana Fm
Kula Fm
FEOT
MGO
0.00
1.50
3.00
4.50
6.00
7.50
9.00
10.50
12.00
13.50
15.00
15.87
13.89
11.91
9.92
7.94
5.95
3.97
1.98
0.00

Figure 12. Plot of MgO against P_2O_5.

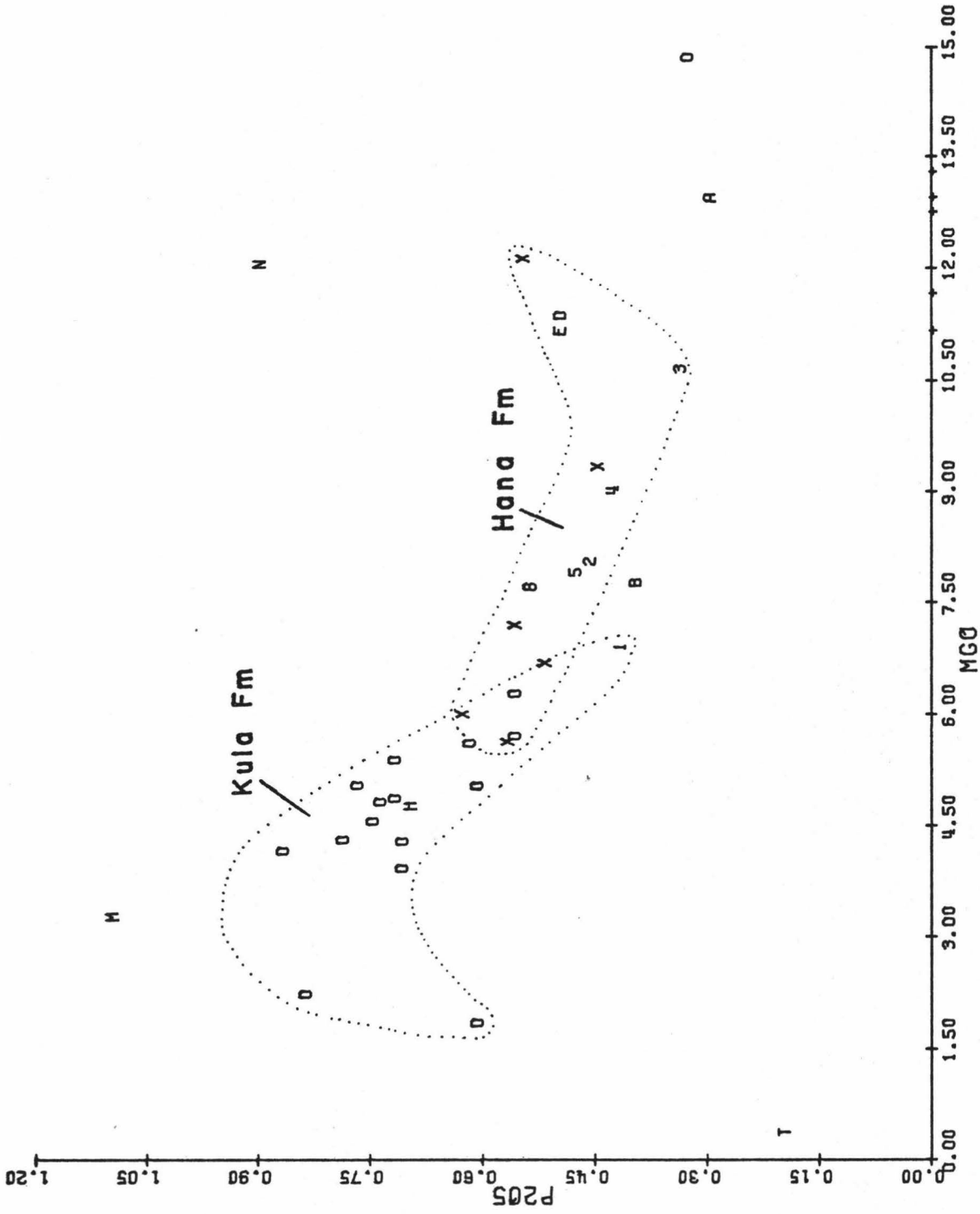
Kula Fm
Hana Fm
P2O5
MGO
0.00
0.15
0.30
0.45
0.60
0.75
0.90
1.05
1.20
1.50
3.00
4.50
6.00
7.50
9.00
10.50
12.00
13.50
15.00

Figure 13. Plot of MgO against TiO_2.

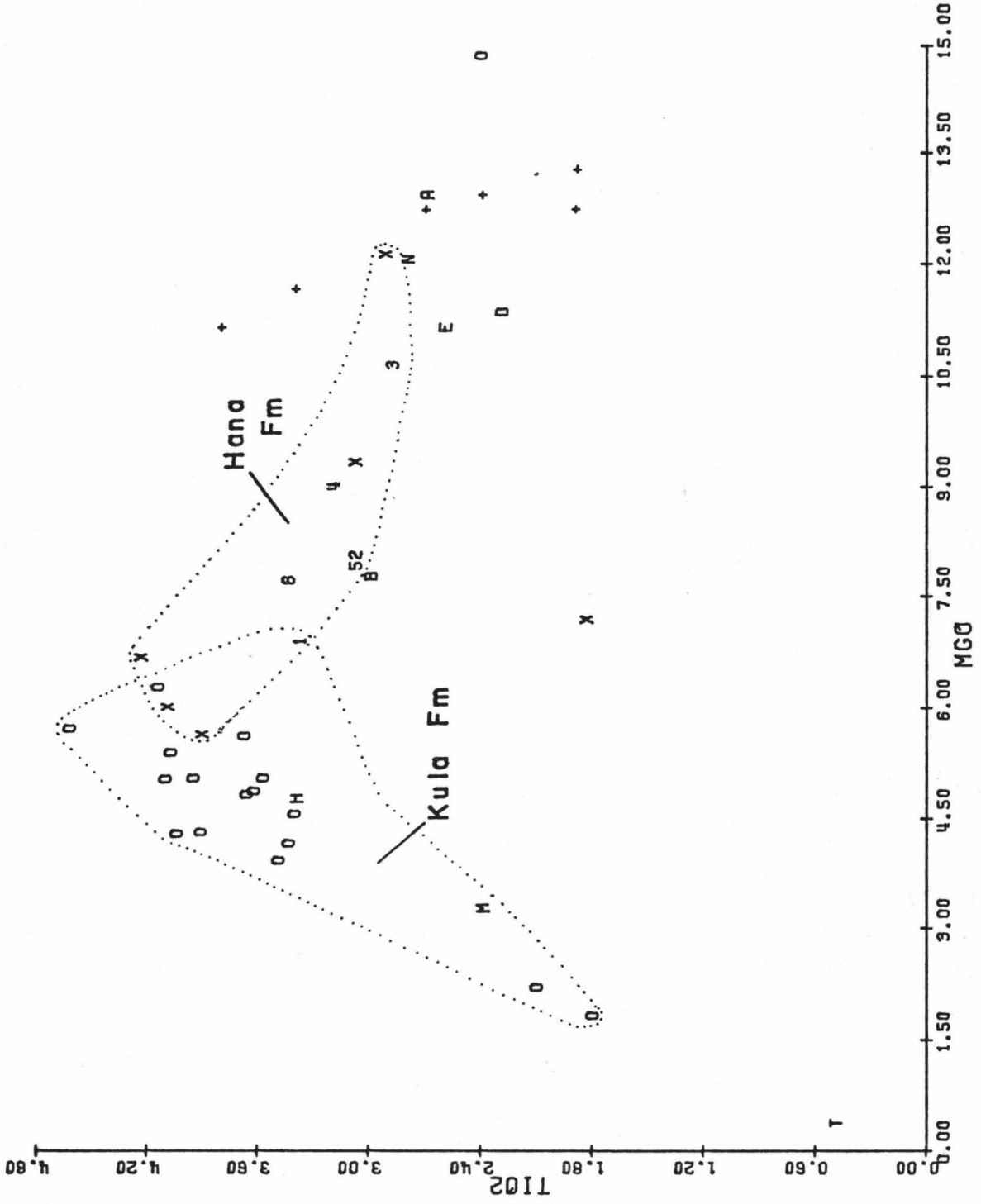
Hana
Fm
Kula Fm
TiO2
MgO
0.00
0.60
1.20
1.80
2.40
3.00
3.60
4.20
4.80
1.50
3.00
4.50
6.00
7.50
9.00
10.50
12.00
13.50
15.00

Figure 14. Plot of MgO against SiO_2.

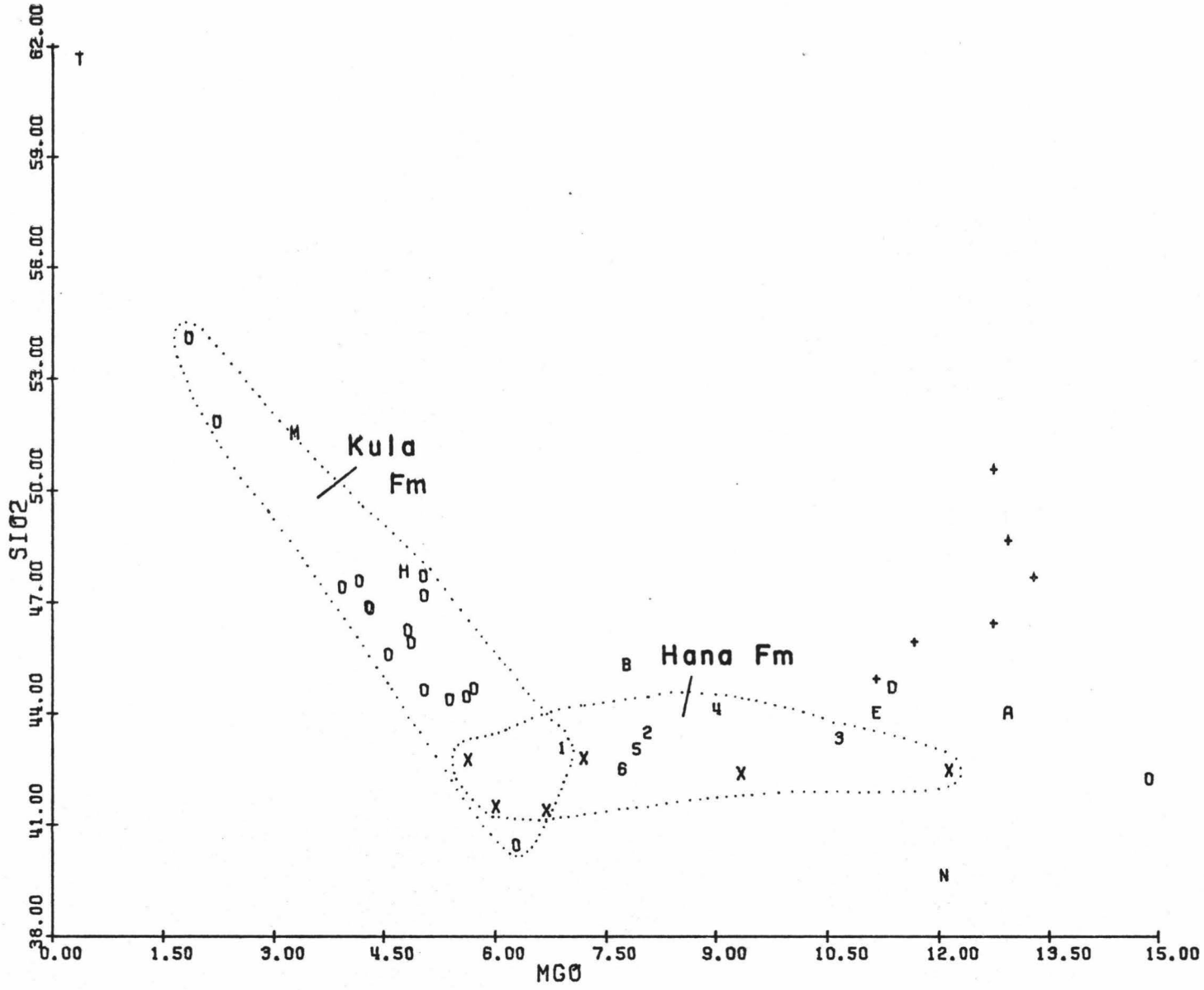
SIØ2
MGØ
62.00
59.00
56.00
53.00
50.00
47.00
44.00
41.00
38.00
0.00
1.50
3.00
4.50
6.00
7.50
9.00
10.50
12.00
13.50
15.00
Kula
Fm
Hana Fm

Figure 15. Plot of MgO against Al_2O_3.

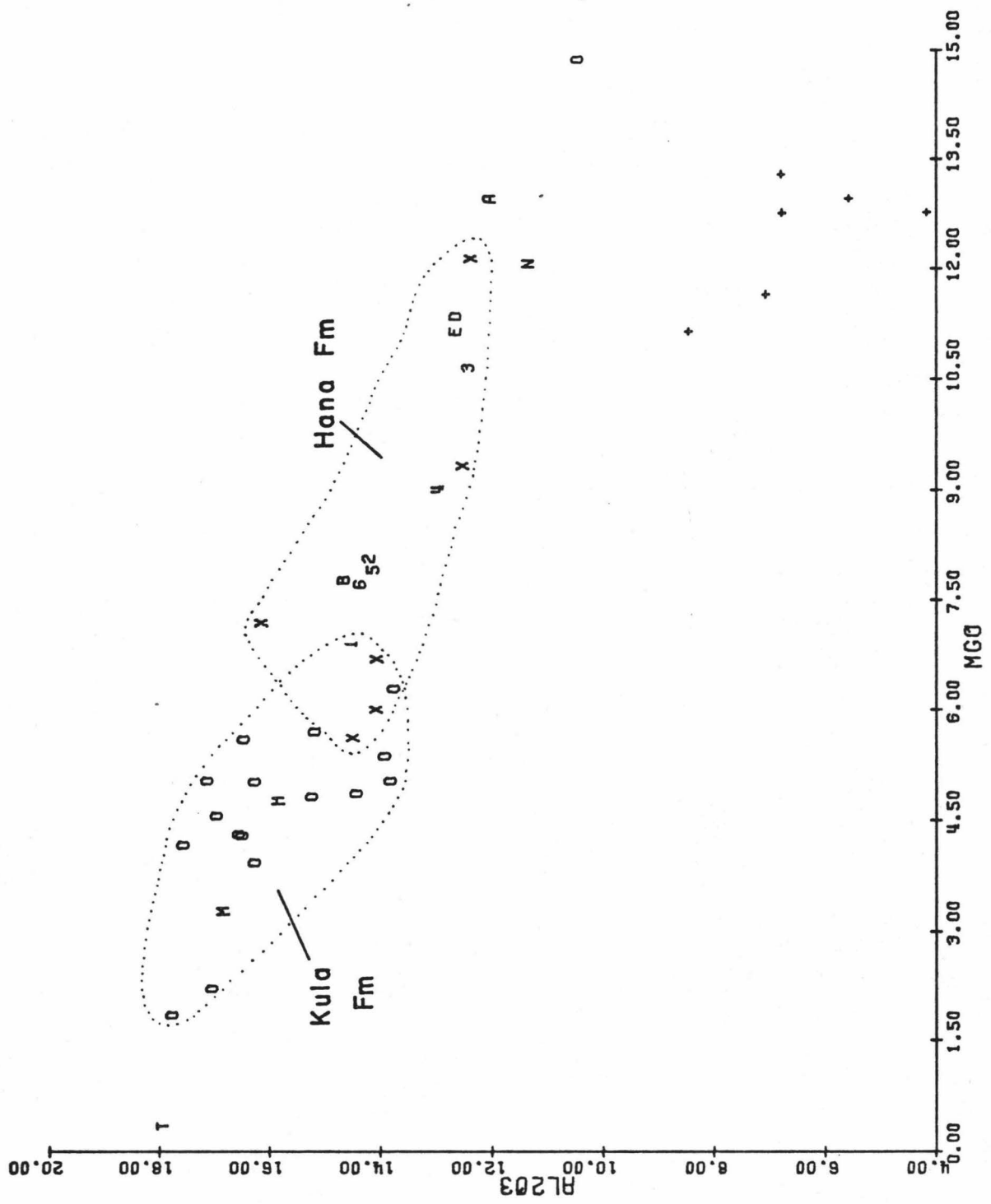
Hana Fm
Kula Fm
AL2O3
MGO
0.00
1.50
3.00
4.50
6.00
7.50
9.00
10.50
12.00
13.50
15.00
4.00
6.00
8.00
10.00
12.00
14.00
16.00
18.00
20.00

LITERATURE CITED

Bloss, F.D., 1961, An Introduction to the Methods of Optical Crystallography, Holt, Reinhart and Winston, New York, 294 pp.

Bowen, R.W., 1971, Graphic normative analysis program: National Technical Information Service, PB 206 736, Springfield, Va. 22151, 80 pp.

Brill, Richard C., 1975, The Geology of the Lower Southwest Rift of Haleakala, Hawaii, Unpublished M.S. thesis, University of Hawaii, 65 pp.

Bryan, W.B., 1972, Morphology of quench crystals in submarine basalts, Jour. Geophys. Research, v. 77, p. 5812-5819.

Climates of the States, Volume II-Western States, National Oceanic and Atmospheric Administration, Washington, 1974.

Climatic Summary of Hawaii-Supplement for 1919 through 1952, U.S. Weather Bureau, Washington, 1953.

Cross, W., 1915, Lavas of Hawaii and their relations, U.S.G.S. Prof. Paper 88, 97 pp.

Dana, E.S., 1889, Contributions to the petrography of the Sandwich Islands, Am. Jour. Sci. Ser. 3, v. 37, p. 441-467.

Dana, J.D., 1849, United States Exploring Expedition 1838-42, v. 10, Geology, p. 226-231.

Fodor, R.V., K. Keil, and T.E. Bunch, 1975, Contributions to the mineral chemistry of Hawaiian rocks. IV. Pyroxenes in rocks from Haleakala and West Maui Volcanoes, Maui, Hawaii, Contrib. Mineral. Petrol., v. 50, p. 173-195.

George, W.O., 1924, The relation of the physical properties of natural glasses to their chemical composition, Jour. Geol., v. 32, p. 353-372.

Green, D.H., 1969, The origin of basaltic and nephelinitic magmas in the earth's mantle, Tectonophysics, v. 7, p. 409-422.

Heinrich, E.W., 1965, Microscopic Identification of Minerals, McGraw-Hill Co., New York, 414 pp.

Johannsen, A., 1931, A Descriptive Petrography of the Igneous Rocks, v. 1, University of Chicago Press, 267 pp.

Johnston-Lavis, H.J., 1885-86, On the fragmentary ejectamenta of volcanoes, Geol. Assoc. London Proc., v. 9, p. 421-432.

Keil, K., R.V. Fodor, and T.E. Bunch, 1972, Contributions to the mineral chemistry of Hawaiian Rocks. II. Feldspars and interstitial material in rocks from Haleakala and West Maui Volcanoes, Maui, Hawaii, Contrib. Mineral. Petrol., v. 37, p. 253-276.

Kushiro, I., 1965, The liquidus relations in the systems forsterite-$CaAl_2SiO_6$-Silica and forsterite-nepheline-silica at high pressures, Carnegie Inst. Wash. Year Book, v. 64, p. 103-109.

_____, 1969, The system forsterite-diopside-silica with and without water at high pressures, Am. Jour. Sci., v. 267-A, Schairer v., p. 269-294.

_____, 1975, On the nature of silicate melt and its significance in magma genesis: regularities in the shift of the liquidus boundaries involving olivine, pyroxene, and silica minerals, Am. Jour. Sci., v. 275, p. 411-431.

Macdonald, G.A., 1942, Potash-oligoclase in Hawaiian lavas, Am. Mineralogist, v. 27, p. 793-800.

_____, 1968, Composition and origin of Hawaiian lavas, Geol. Soc. America Mem. 116, p. 477-522.

Macdonald, G.A., and T. Katsura, 1962, Relationship of Petrographic Suites in Hawaii, Amer. Geoph. Un. Monog. 6, p. 187-195.

_____, 1964, Chemical Composition of Hawaiian Lavas, Jour. Petrology, v. 5, p. 82-133.

_____, 1965, Eruption of Lassen Peak, Cascade Range, California, in 1915: example of mixed magmas, Geol. Soc. American Bull., v. 76, p. 475-482.

Madconald, G.A., and H.A. Powers, 1946, Contribution to the Petrography of Haleakala Volcano, Hawaii, Geol. Soc. American Bull., v. 57, p. 115-124.

_____, 1968, A Further Contribution to the Petrology of Haleakala Volcano, Hawaii, Geol. Soc. American Bull., v. 79, p. 877-888.

McDougall, I., 1964 "Potassium-Argon age from lavas of the Hawaiian Islands," Geol. Soc. America Bull., v. 77, p. 107-128.

Möhle, F., 1902, Beitrag zur petrographie der Sandwich- und Samoa-Inseln, Neues Jahrb. Beil. Bd., v. 15, p. 66-194.

Oostdam, B.L., 1965, Age of lava flows on Haleakala, Maui, Hawaii, Geol. Soc. America Bull., v. 76, p. 393-394.

Powers, H.A., 1935, Differentiation of Hawaiian lavas, Am. Jour. Sci. 5th ser., v. 30, p. 57-71.

Powers, S., 1920, Notes on Hawaiian petrology, Am. Jour. Sci., v. 50, p. 256-280.

Reber, G., 1959, Age of lava flows on Haleakala, Hawaii, Geol. Soc. American Bull., v. 70, p. 1245-1246.

Stearns, H.T., and G.A. Macdonald, 1942, Geology and ground-water resources of the island of Maui, Hawaii, Hawaii Div. Hydrog. Bull. 7, 344 pp.

Tröger, W.E., 1971, Optische Bestimmung der gestcinsbildenden Minerale, E. Schweizerbart'sche Verlagsbuchhandlung, Stuttgart, 188 pp.

Vogl, R.J., 1971, General ecology of the northeast outerslopes of Haleakala Crater, East Maui, Hawaii, Contributions from the Nature Conservancy, no. 6, p. 1-8.

Washington, H.S., and H.E. Merwin, 1922, Augite of Haleakala, Maui, Hawaiian Islands, Am. Jour. Sci., 5th ser., v. 3, p. 117-122.

Yoder, H.S., Jr., and C.E. Tilley, 1961, Simple basalt systems, Carnegie Inst. Wash. Year Book, v. 60, p. 106-113.

_____, 1962, Origin of basalt magmas: An experimental study of natural and synthetic rock systems, Jour. Petrology, v. 3, p. 342-532.

Plate 1. Geologic map of the upper southwest rift zone of Haleakala.